file 13-503

8417

P
91
C654
M37
1972-
1974
v.2

Report No. 2 to

Department of Supply and Services, Ottawa

on Contract No. 01GR.36100-2-0204

Serial No. 0GR2-0163

(2) PROPAGATION CHARACTERISTICS OF OPTICAL FIBRES

Covering Period April 1, 1972 to April 30, 1973

G.L. Yip and (1) J. Martucci

Department of Electrical Engineering

McGill University,

Montreal, Quebec.

Prepared for

Communications Research Centre

Shirley Bay, Ottawa, Ontario

May, 1973.

Industry Canada
Library - Queen
AOUT AUG 16 2012
Industrie Canada
Bibliothèque - Queen

COMMUNICATIONS CANADA
JUIN JUNE 22 1984
LIBRARY – BIBLIOTHÈQUE

P
91
C65V
M37
1972-74
V.2

DD545917
DL545997

checked 11/83

ABSTRACT

Propagation characteristics of the cladded fibre are reported for a cladding to core ratio (b/a = 20) of twenty; this is suitable for single mode operation. Mode control by an absorption jacket is treated in some detail. Power lost from discrete scattering centres (on or very near fibre axis), as well as intrinsic fibre absorption loss is investigated.

INTRODUCTION

As stated in Report 1 (CRC), all results presented therein were done for "leaking" modes with a cladding to core ratio ($\bar{r} = b/a = 2$) of two. This ratio is appropriate for the design of a multimode fibre. For single mode operation, a more practical ratio is about 15 or 20.

We now report propagation characteristics for a ratio of 20 covering the complete mode spectrum, i.e. "leaky" and "propagating" modes. The effect of cladding thickness on the modes is also investigated.

A study into the loss characteristics of the fibre is also made. Attenuation curves for intrinsic fibre absorption loss as well as for "mode control" (absorption jacket) are presented. Finally, we treat the power loss due to scattering from fibre impurities on or very near the fibre axis.

TABLE OF CONTENTS

PART I

PROPAGATION CHARACTERISTICS OF CLADDED FIBRE

1. Complete Mode Spectrum

A. Physical Picture of the Different Modes. (see Fig. 1).

When the cladded fibre is excited by a launching device (LASER) or guided waves encounter scattering centres in the fibre, there are three types of modes that have to be considered:

(i) Radiating Modes: $0 \leq \bar{\beta} \leq 1$ (continuous spectrum)

These modes leak out into the outer region (n_3), and hence are not guided by the fibre.

(ii) Guided Modes:

(a) "Leaking" Modes: $1 \leq \bar{\beta} \leq n_2$

These modes leak out into the cladding, but get totally reflected at the cladding-air interface.

(b) "Propagating" Modes: $n_2 \leq \bar{\beta} \leq n_1$

These modes do not leak out into the cladding, since total internal reflection occurs at the core-cladding interface.

CLADDED OPTICAL FIBRE

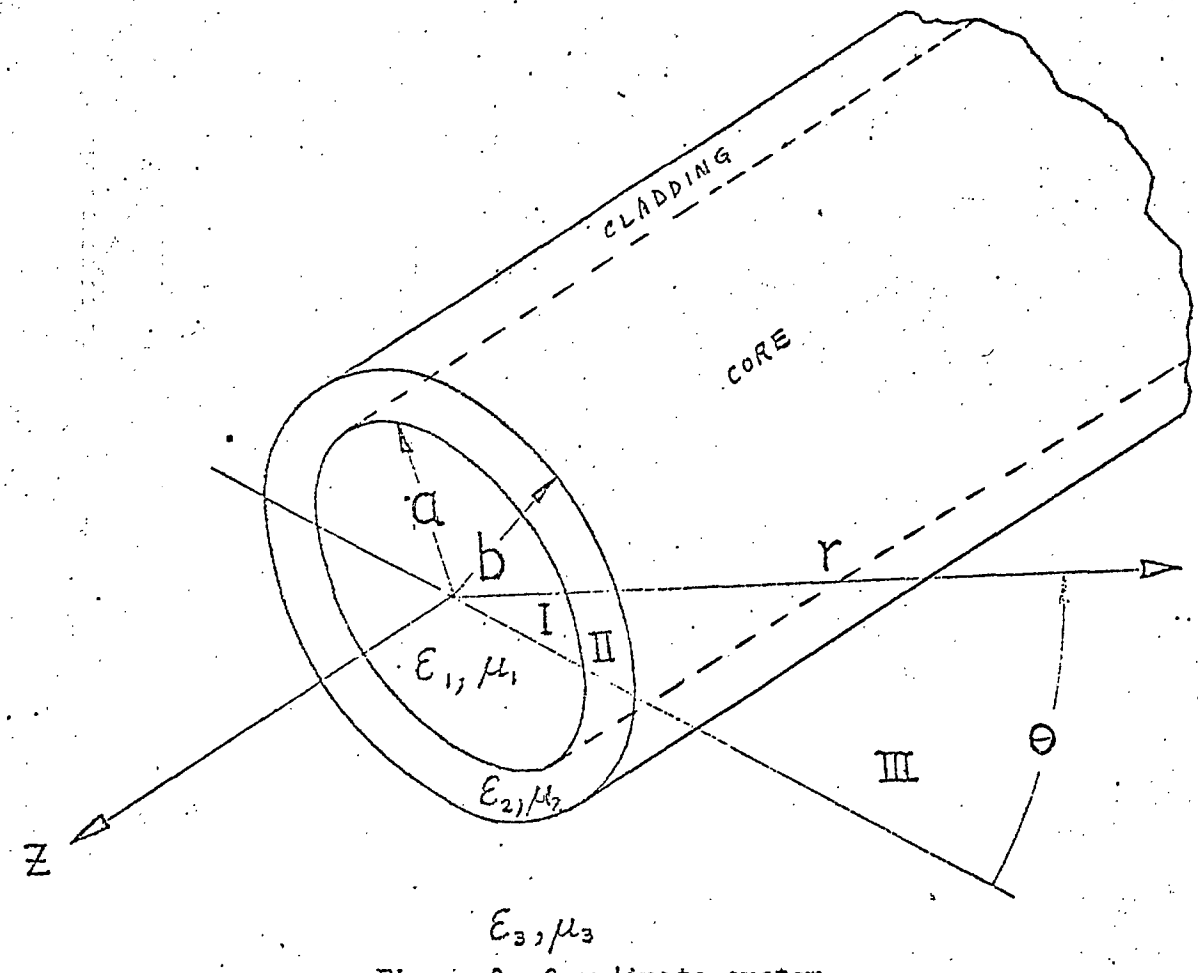

Figure 0. Coordinate system

PHYSICAL PICTURE OF DIFFERENT MODES

Radiating Mode

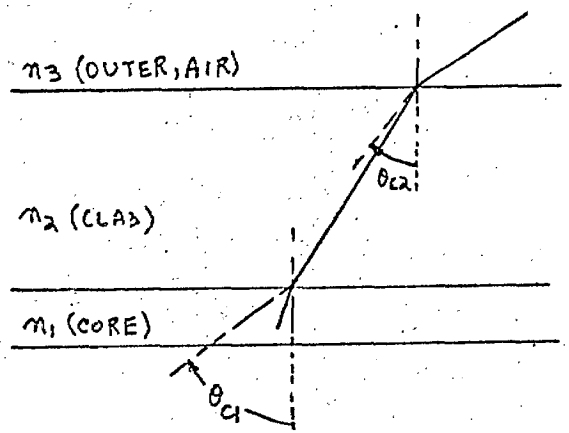

Core-Cladding Critical Angle $\}$ $\sin\theta_{C1} = (\frac{n_2}{n_1})$

Cladding-Air Critical Angle $\}$ $\sin\theta_{C2} = (\frac{n_3}{n_2})$

There is transmission through all three regions.

"Leaky" Mode (or cladding mode)

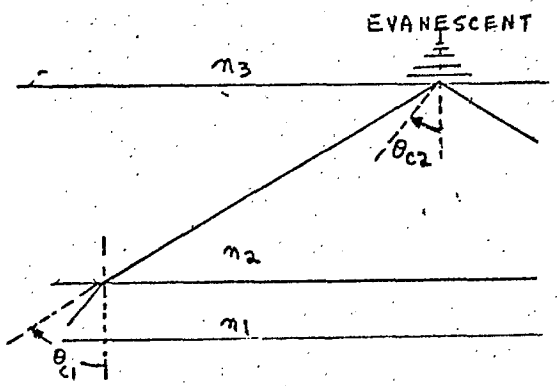

There is "TOTAL INTERNAL REFLECTION" at the cladding-air interface. But there is transmission (LEAKY) through the core-cladding interface.

"Propagating" Mode (or core mode)

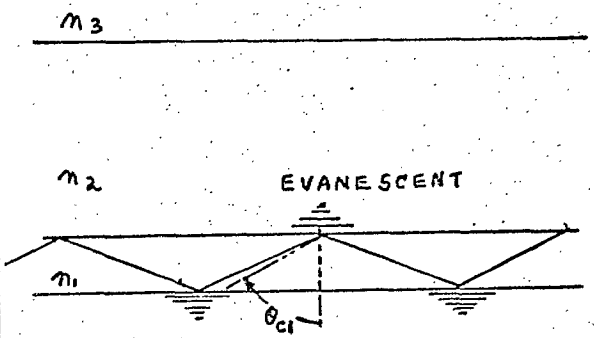

There is "TOTAL INTERNAL REFLECTION" at core-cladding interface. All power is reflected into core, with evanescent wave in cladding.

FIGURE 1

B. Dispersion Curves for the Modes

In what follows all quantities are plotted against normalized frequency, i.e. $V = 2\pi \left(\frac{a}{\lambda_0}\right) \sqrt{\bar{\epsilon}_1 - \bar{\epsilon}_2}$, since it occurs frequently in optical waveguides literature.

Fig. 2a illustrates the continuous radiation region and the "leaky" modes.

Fig. 2b illustrates the transition from "leaky" modes to "propagating" modes.

In both cases the parameters used are:

$(b/a) = 20$

$\bar{\epsilon}_1 = 2.34, \ \bar{\epsilon}_2 = 2.25, \ \bar{\epsilon}_3 = 1.0$

$n_1 = \sqrt{\bar{\epsilon}_1} = 1.53, \ n_2 = \sqrt{\bar{\epsilon}_2} = 1.5$

In Fig. 3 we combine Fig. 2a and Fig. 2b into one page for easy reference.

Hence we have:

"Leaky" region: $1 \leq \bar{\beta} \leq n_2 = 1.5$

"Propagating" region: $n_2 \leq \bar{\beta} \leq n_1 = 1.53$

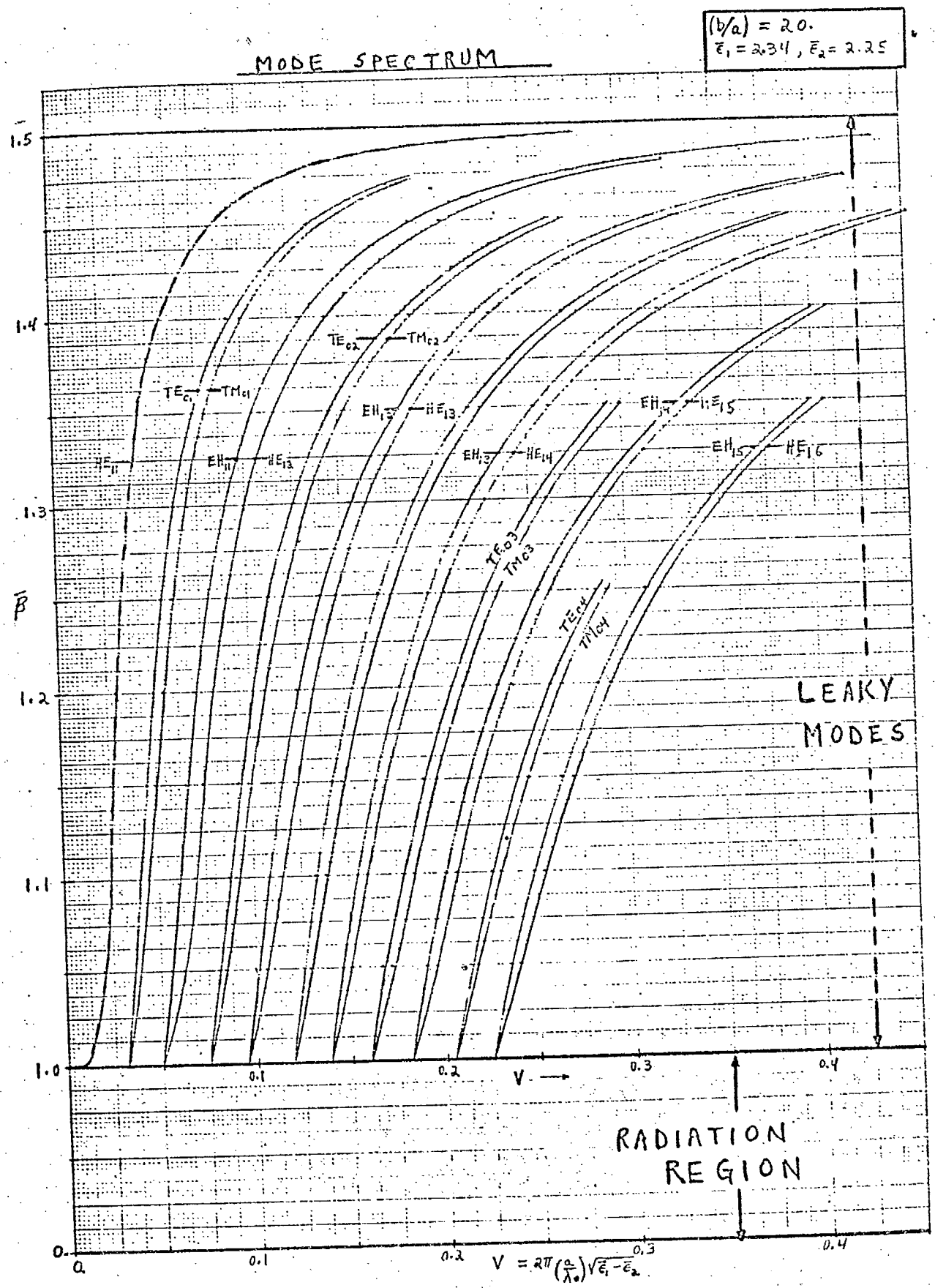
MODE SPECTRUM
(b/a) = 20.
ε̄₁ = 2.34 , ε̄₂ = 2.25
β̄
V →
V = 2π (a/λ₀) √(ε̄₁ − ε̄₂)
TE₀₁
TM₀₁
HE₁₁
EH₁₁
HE₁₂
TE₀₂
TM₀₂
EH₁₂
HE₁₃
EH₂₁
HE₂₂
EH₁₃
HE₁₄
TE₀₃
TM₀₃
EH₂₂
HE₂₃
EH₁₄
HE₁₅
TE₀₄
TM₀₄
EH₂₃
HE₂₄
EH₁₅
HE₁₆
LEAKY MODES
RADIATION REGION
1.5
1.4
1.3
1.2
1.1
1.0
0
0.1
0.2
0.3
0.4

Fig. 2a

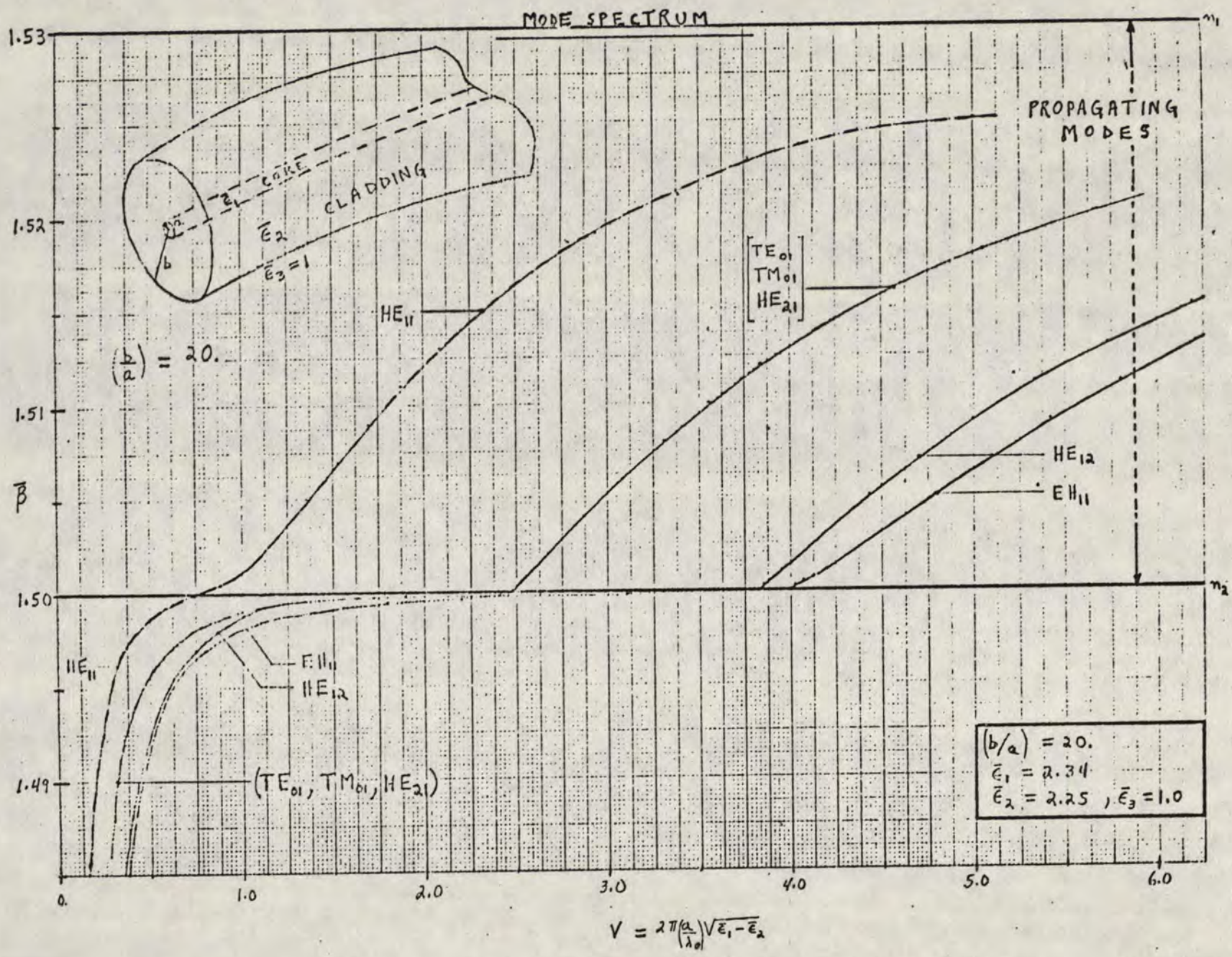
MODE SPECTRUM
1.53
1.52
1.51
1.50
1.49
$\bar{\beta}$
n_1
n_2
PROPAGATING MODES
CLADDING
$\bar{\epsilon}_1$ CORE
$\bar{\epsilon}_2$
$\bar{\epsilon}_3 = 1$
a
b
$\left(\frac{b}{a}\right) = 20.$
HE_{11}
$\begin{bmatrix} TE_{01} \\ TM_{01} \\ HE_{21} \end{bmatrix}$
HE_{12}
EH_{11}
$\left(TE_{01}, TM_{01}, HE_{21}\right)$
$\left(b/a\right) = 20.$
$\bar{\epsilon}_1 = 2.34$
$\bar{\epsilon}_2 = 2.25$, $\bar{\epsilon}_3 = 1.0$
0.
1.0
2.0
3.0
4.0
5.0
6.0
$V = 2\pi\left(\frac{a}{\lambda_0}\right)\sqrt{\bar{\epsilon}_1 - \bar{\epsilon}_2}$

FIG. 21

MODE SPECTRUM

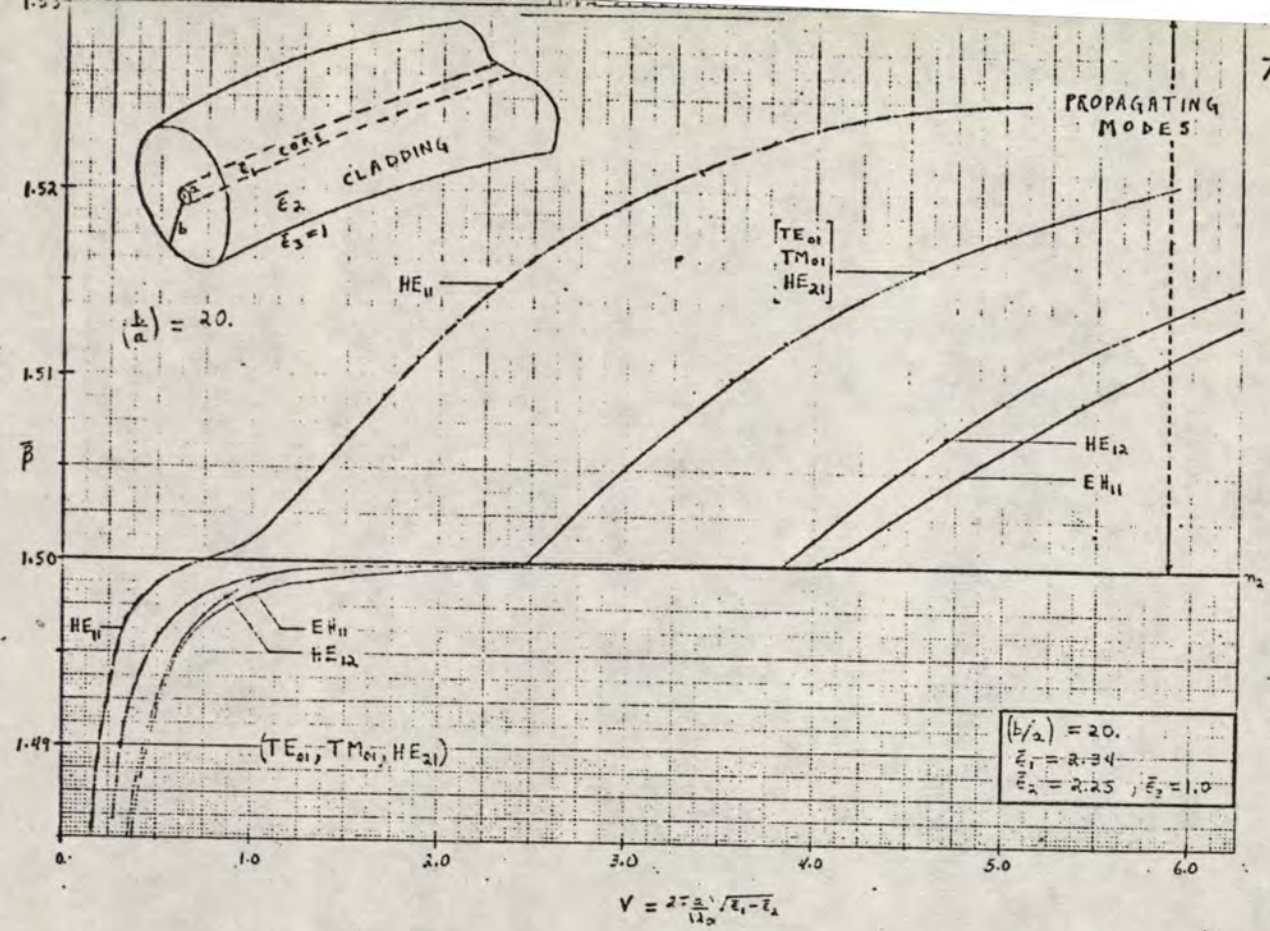

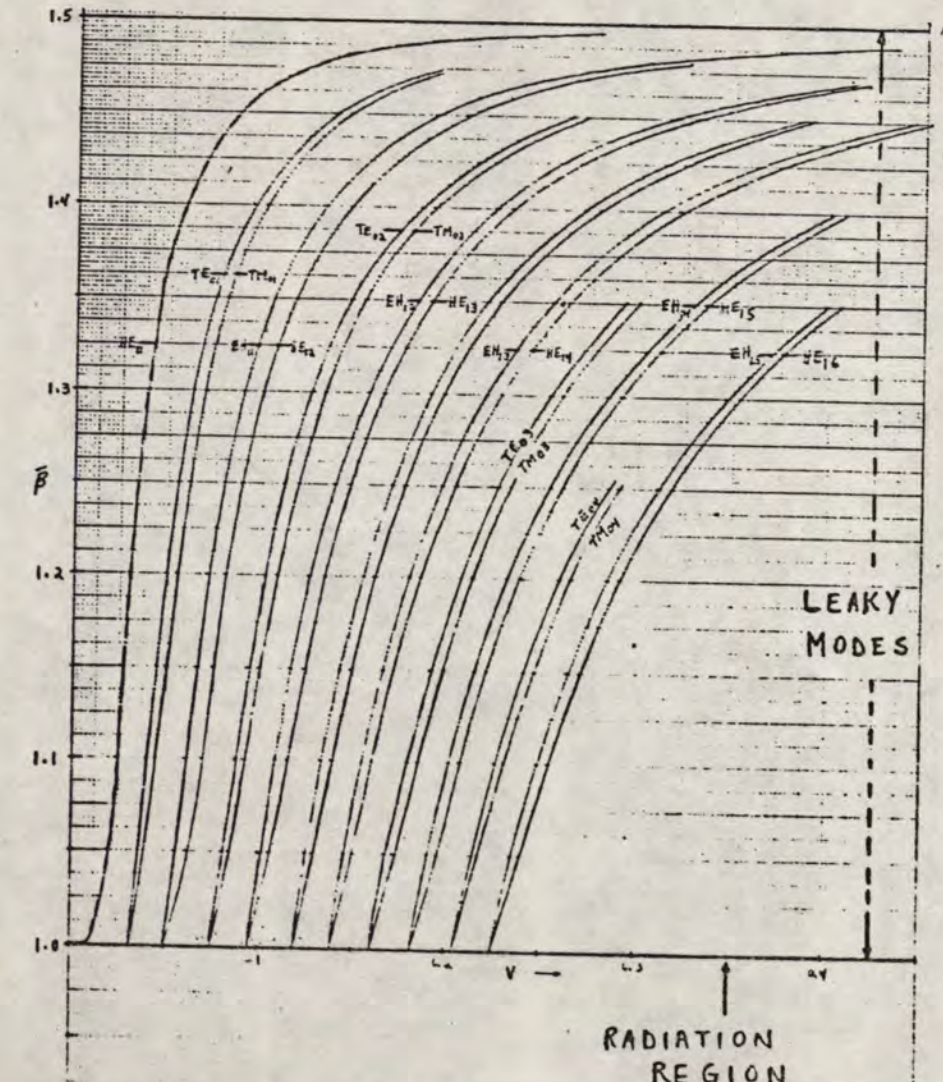

FIG. 3

2. Effect of Cladding Thickness on the Modes

In Fig. 4, we show how the dispersion curves change as the cladding thickness is varied.

(a) Infinite Cladding: (rod solution): $(b/a) = \infty$

These curves lie between n_1 and n_2, i.e. $n_2 \leq \bar{\beta} \leq n_1$. HE_{11} has no low frequency cut-off. TE_{01}, TM_{01}, HE_{21} overlap into one. EH_{11} and HE_{12} have the same cut-off value.

(b) Finite Cladding:

(i) $(b/a) = 20$: All the modes in the "leaky" region merge very fast into the rod solution $(b/a = \infty)$, but now EH_{11} and HE_{12} have different "transition" values.

(ii) $(b/a) = 5$: For HE_{11} there is a more pronounced difference between the rod solution and $(b/a) = 5$; however, the set of modes TE_{01}, TM_{01}, HE_{21} EH_{11}, HE_{12} still merge quite rapidly into the rod solution.

From Fig. 4, we observe that changing the ratio $(b/a) = 5$ to 20 "squeezes" the "leaky" modes close to the origin, without affecting the "propagating" modes very much. As $(b/a) \to \infty$, the "leaky" modes are brought virtually to non-existence, (as expected).

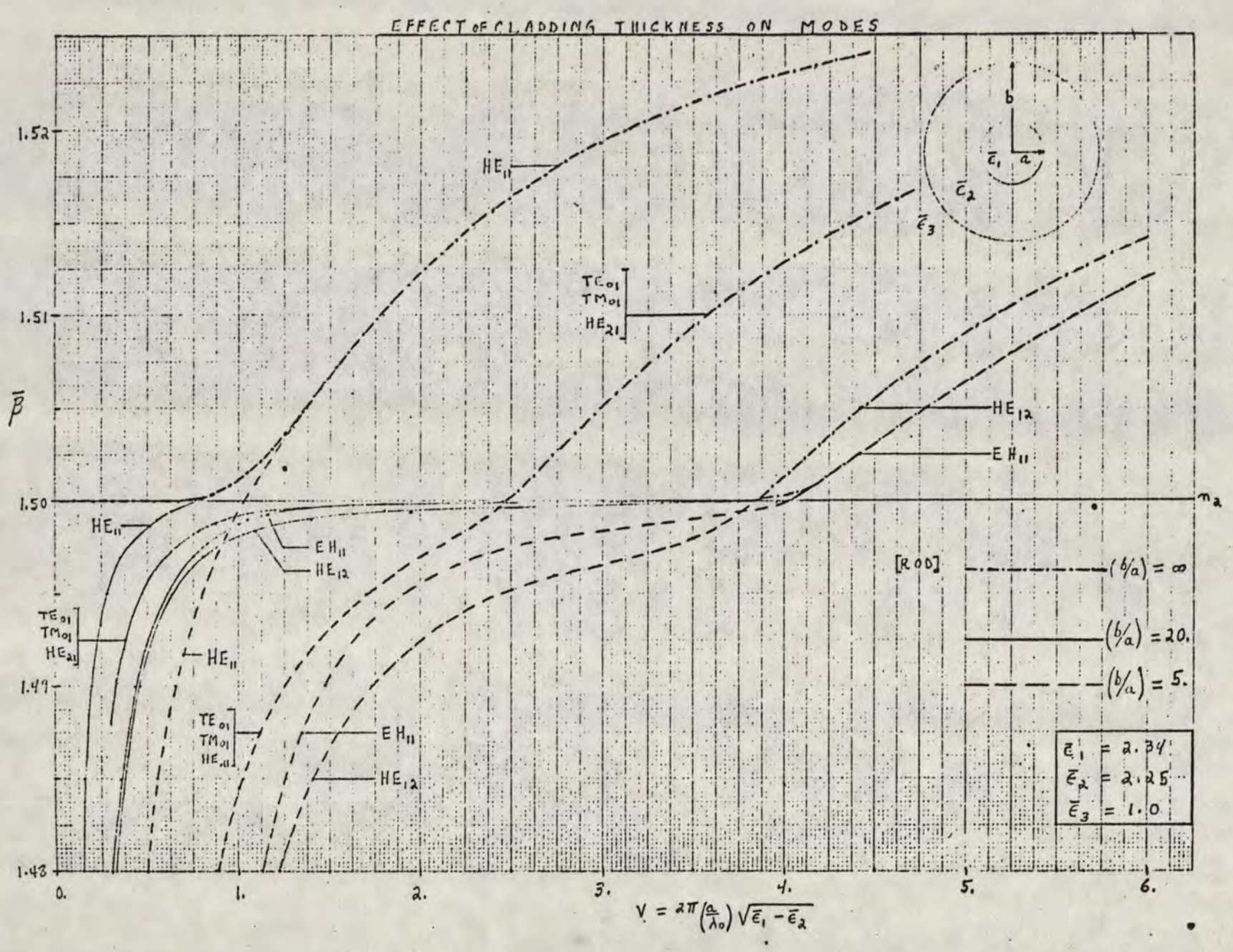
EFFECT OF CLADDING THICKNESS ON MODES
1.52
1.51
1.50
1.49
1.48
$\bar{\beta}$
0.
1.
2.
3.
4.
5.
6.
$V = 2\pi\left(\frac{a}{\lambda_0}\right)\sqrt{\bar{\epsilon}_1 - \bar{\epsilon}_2}$
n_2
HE11
TE01
TM01
HE21
EH11
HE12
[ROD]
$(b/a) = \infty$
$(b/a) = 20.$
$(b/a) = 5.$
$\bar{\epsilon}_1 = 2.34$
$\bar{\epsilon}_2 = 2.25$
$\bar{\epsilon}_3 = 1.0$
b
a
$\bar{\epsilon}_1$
$\bar{\epsilon}_2$
$\bar{\epsilon}_3$

Fig. 4

3. Phase Velocity and Group Velocity

(a) Phase Velocity: (v_p)

In this report we have plotted

$$\bar{\beta} = \left(\frac{\beta}{k_0}\right) \text{ v s. } \quad V = 2\pi \left(\frac{a}{\lambda_0}\right) \sqrt{\bar{\epsilon}_1 - \bar{\epsilon}_2},$$

where

$$k_0 = (2\pi / \lambda_0)$$

$$v_p = \frac{\omega}{\beta} = \frac{k_0}{(\bar{\beta})} \frac{v_0}{k_0} = \frac{v_0}{\bar{\beta}} \quad , \text{ USING } \begin{cases} \omega = k_0 v_0 \\ \beta = \bar{\beta} k_0 \end{cases}$$

$$\therefore \frac{v_p}{v_0} = \frac{1}{\bar{\beta}} \qquad \text{normalized phase velocity} \qquad (1.1)$$

(b) Group Velocity: (v_g)

Group velocity has been calculated by the power and energy method, i.e.

$$v_g = \frac{P(\bar{\beta}, V)}{W(\bar{\beta}, V)} = \frac{\text{total axial power flow}}{\text{total energy stored per unit length}}$$

$P_i(\bar{\beta}, V)$, $W_i(\bar{\beta}, V)$ are the corresponding quantities in each region of the fibre waveguide.

In Fig. 5 we have replotted the dispersion curves on a semi-log graph paper so that both the leaky and propagating modes could be covered on the V (normalized frequency) scale. However, it is necessary to expand $\bar{\beta}$ scale for the propagating region (i.e. $n_2 \leq \bar{\beta} \leq n_1$).

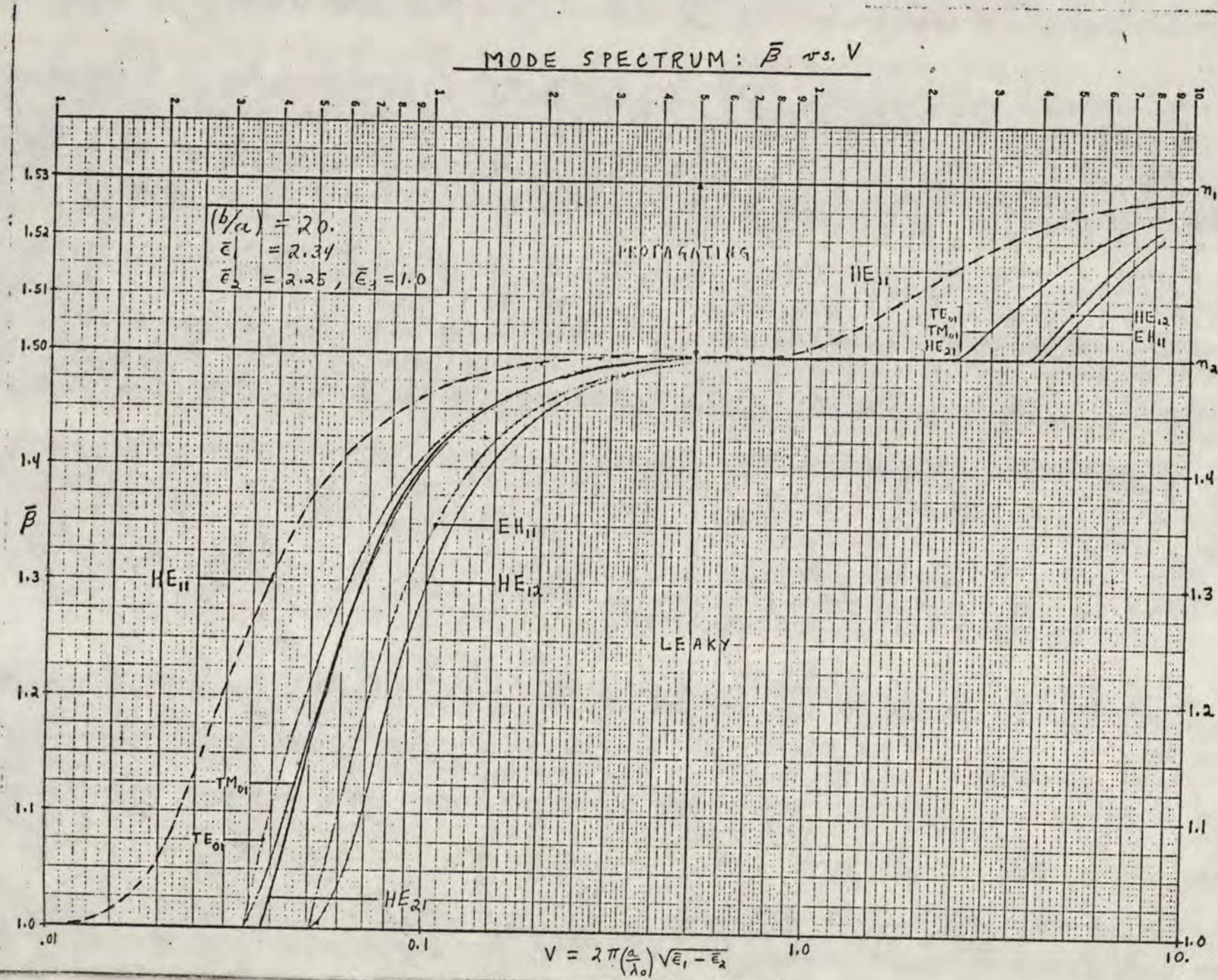
MODE SPECTRUM: $\bar{\beta}$ vs. V
$(b/a) = 20.$
$\bar{\epsilon}_1 = 2.34$
$\bar{\epsilon}_2 = 2.25, \bar{\epsilon}_3 = 1.0$
PROPAGATING
LEAKY
HE_{11}
TE_{01}
TM_{01}
HE_{21}
EH_{11}
HE_{12}
$\bar{\beta}$
$V = 2\pi\left(\frac{a}{\lambda_0}\right)\sqrt{\bar{\epsilon}_1 - \bar{\epsilon}_2}$
n_1
n_2
1.53
1.52
1.51
1.50
1.4
1.3
1.2
1.1
1.0
.01
0.1
1.0
10.

Fig. 5

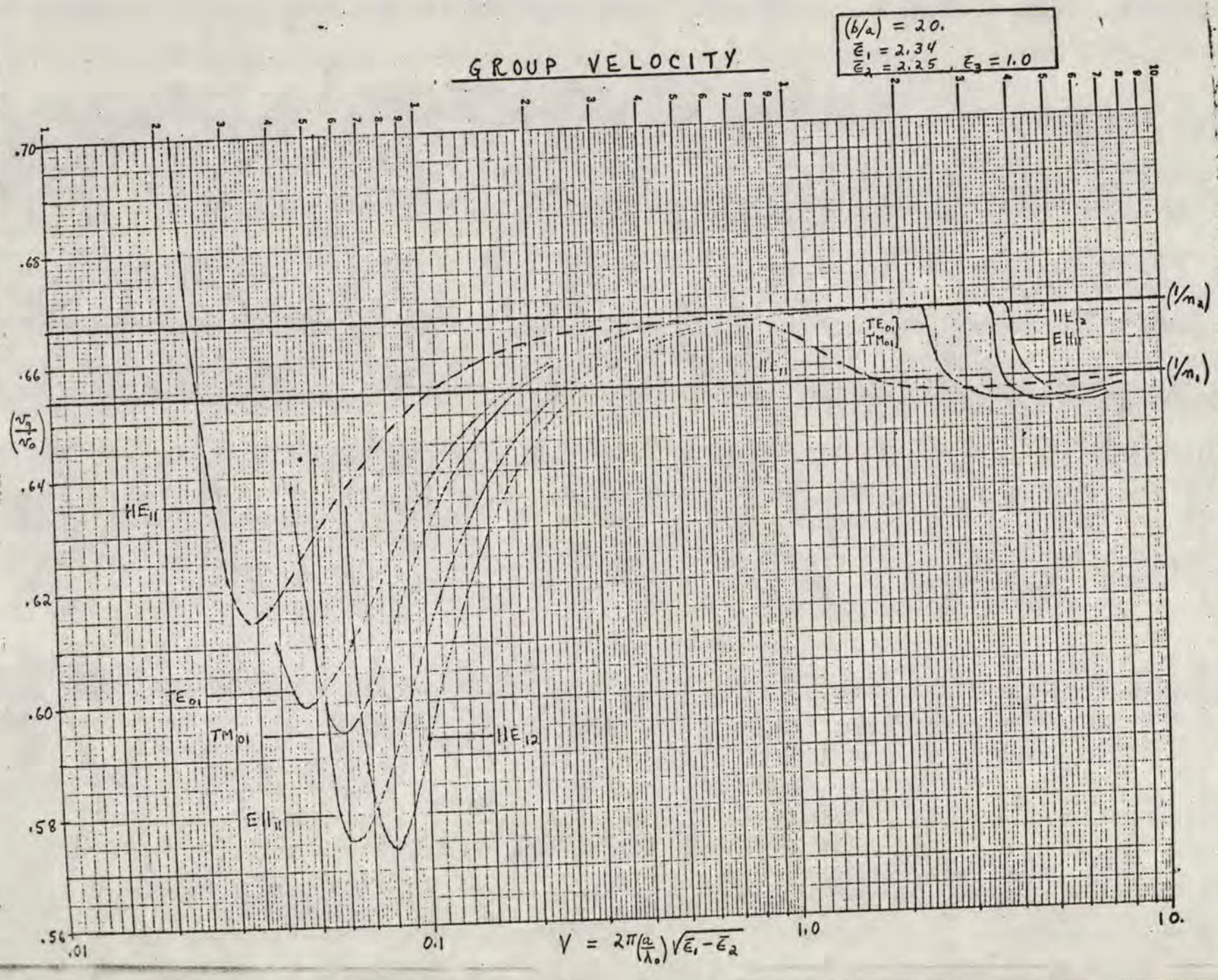
GROUP VELOCITY
(b/a) = 20.
ε̄1 = 2.34
ε̄2 = 2.25 , ε̄3 = 1.0
(1/n2)
(1/n1)
HE11
TE01
TM01
EH11
HE12
HE21
EH11
.70
.68
.66
.64
.62
.60
.58
.56
.01
0.1
1.0
10.
V = 2π(a/λ0)√(ε̄1 − ε̄2)

FIG.

GROUP VELOCITY

$(b/a) = 20.$
$\bar{\epsilon}_1 = 2.34$
$\bar{\epsilon}_2 = 2.25$, $\bar{\epsilon}_3 = 1.0$

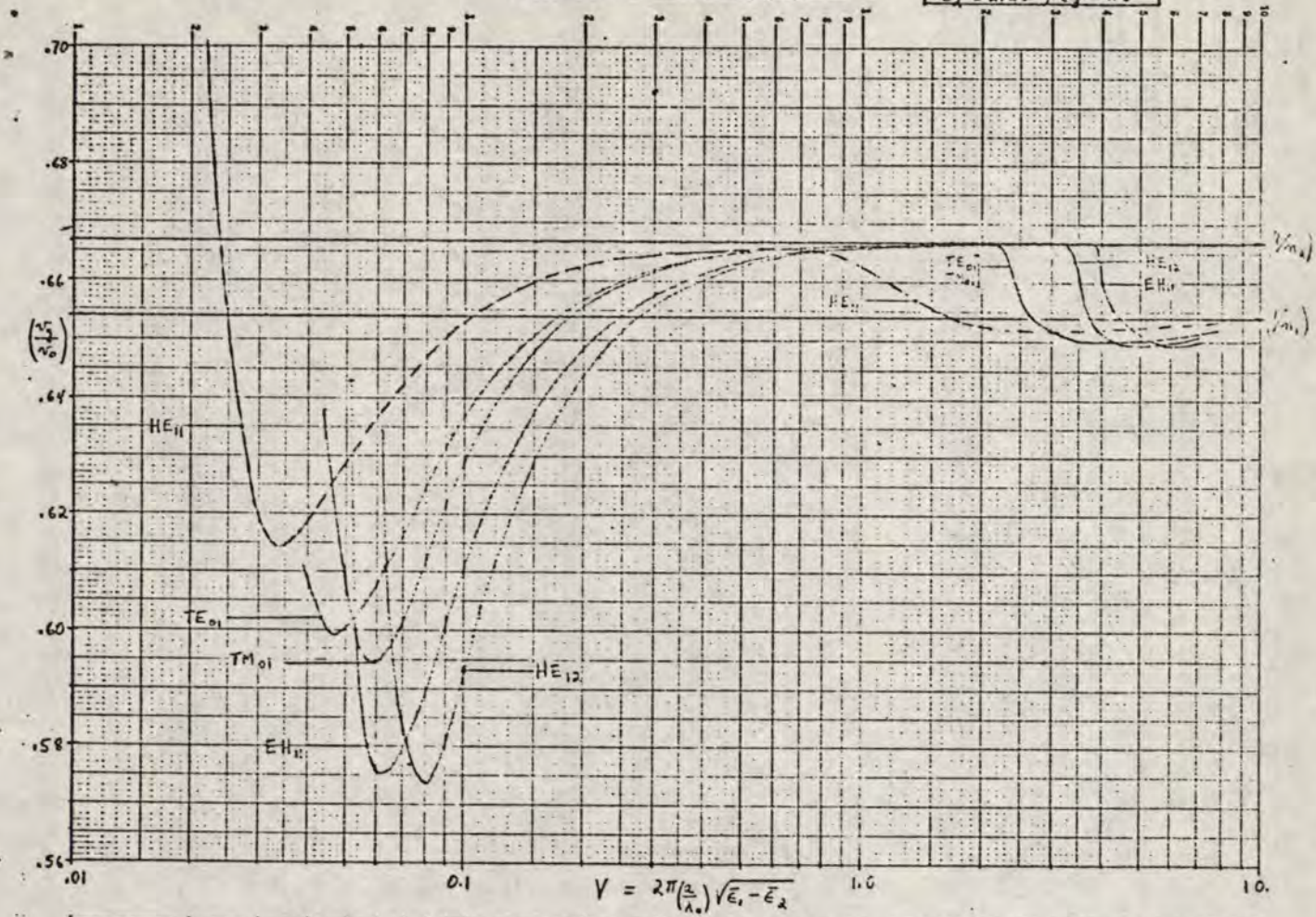

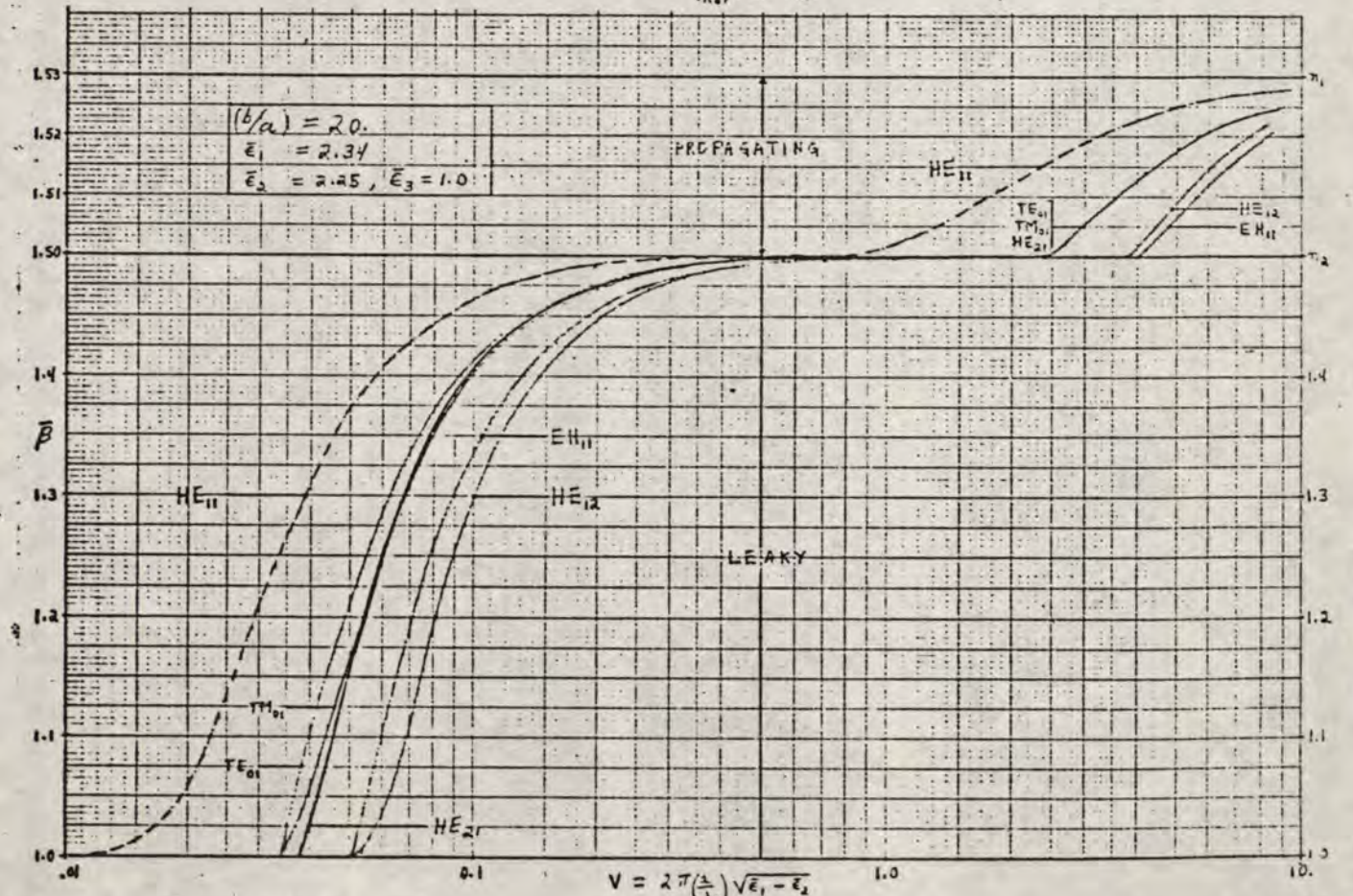

FIG. 7

In Fig. 6 we plot the corresponding group velocity for the various modes. As was stated in Section 2, the dispersion curves for the ratio $(b/a) = 20$ merge very rapidly to the rod solution in the propagating region. Thus, the corresponding group velocity behaves in a similar way.

In Fig. 7, we present the mode spectrum and group velocity on one sheet for easy reference.

4. Concentration of Power vs. Normalized Frequency (V)

Fig. 8 illustrates how the concentration of power changes as we go from the leaky mode region into the propagating mode region.

The total modal power $\underline{P}$ can be represented as

$$P(\bar{\beta},V) = \sum_{i=1}^{3} P_i(\bar{\beta},V)$$

$$= P_1(\bar{\beta},V) + P_2(\bar{\beta},V) + P_3(\bar{\beta},V) \qquad (1.3)$$

[Core] [Cladding] [Outer]

(a) Thus, in Fig. 8a we plot the fraction of power in the core, i.e.,

$$\frac{P_1(\bar{\beta},V)}{P(\bar{\beta},V)} = \underline{\text{vs.}}\ V$$

It is observed that as soon as we enter the propagating region all the power gets concentrated into the core (as expected).

(b) In Fig. 8b we plot the fraction of power in the cladding, i.e.,

$$\frac{P_2(\bar{\beta},V)}{P(\bar{\beta},V)} \quad \underline{\text{vs.}} \quad V$$

We notice that there is a V interval ("bandwidth") where most of the power is concentrated in the cladding. However, when the propagating region is entered, the power in the cladding decays very fast (as expected).

(c) Fig. 9 displays the behaviour of the concentration of power (for HE_{11} mode) from the "leaky" region to the "propagating" region.

At very low frequency (near cut-off of TE_{01}) the power is concentrated in the outer medium, hence

$$\frac{P_3(\bar{\beta},V)}{P(\bar{\beta},V)} > \frac{P_2(\bar{\beta},V)}{P(\bar{\beta},V)} \qquad \text{(cladding)}$$

As we move away from cut-off, the power in the outer medium goes down and gets stored into the cladding "leaky" region).

Then, as soon as the propagating region is entered ($V \simeq .8$ for HE_{11}) the power in the cladding begins to drop and the power in core increases, i.e.,

$(\frac{P_2}{P})$ decays and $(\frac{P_1}{P})$ increases (as expected).

Hence, the power gets transferred from the outer medium into the core as the frequency (V) increases.

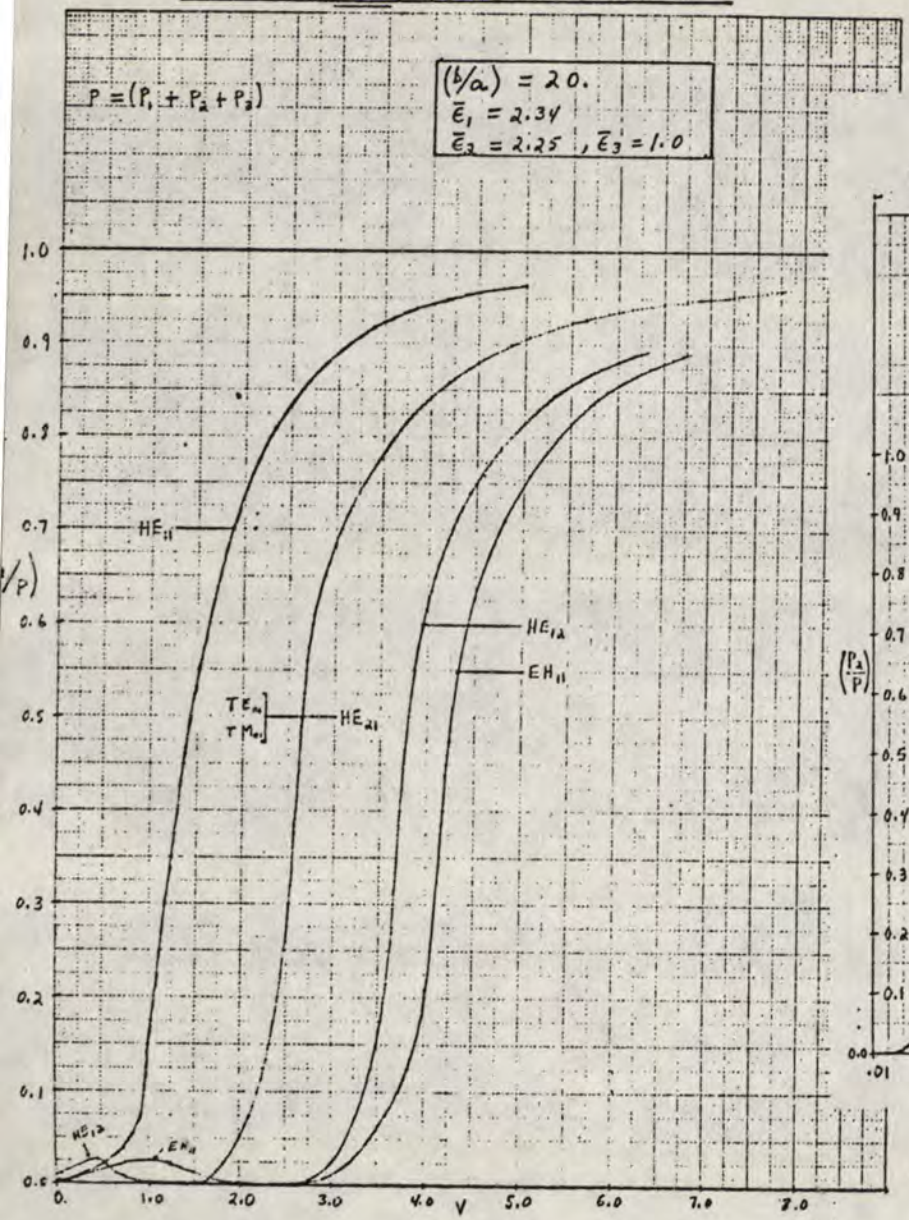
(POWER IN CORE/MODAL POWER) vs. V
P = (P1 + P2 + P3)
(b/a) = 20.
ε̄1 = 2.34
ε̄2 = 2.25 , ε̄3 = 1.0
HE11
HE12
EH11
TE01
TM01
HE21
(P1/P)
V
0.
1.0
2.0
3.0
4.0
5.0
6.0
7.0
8.0

FIG. 8(a)

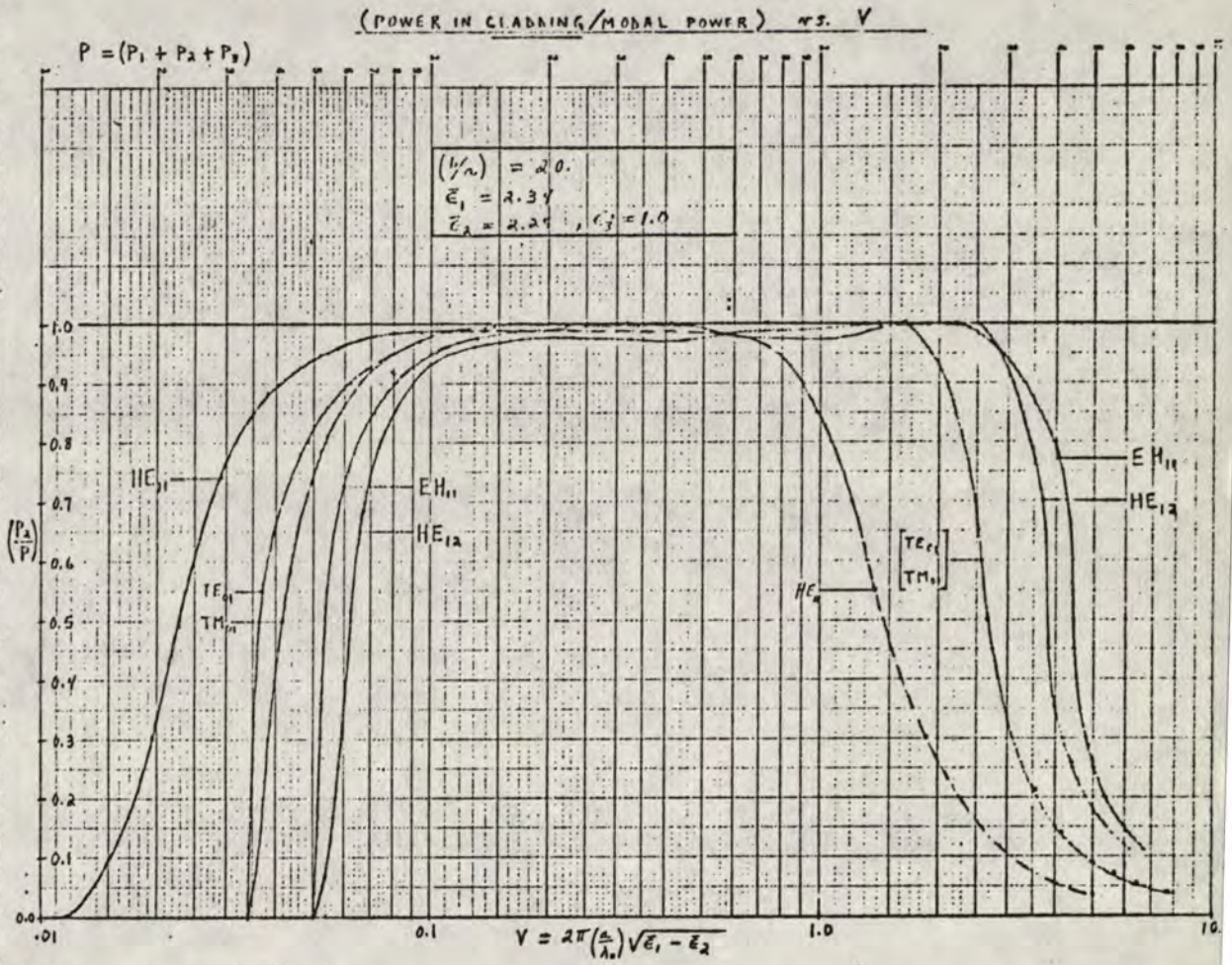
(POWER IN CLADDING/MODAL POWER) vs. V
P = (P1 + P2 + P3)
(b/a) = 20.
ε̄1 = 2.34
ε̄2 = 2.25 , ε̄3 = 1.0
HE11
EH11
HE12
TE01
TM01
HE21
TE11
TM11
EH11
HE12
(P2/P)
V = 2π(a/λ0)√(ε̄1 − ε̄2)
.01
0.1
1.0
10.

FIG. 8(b)

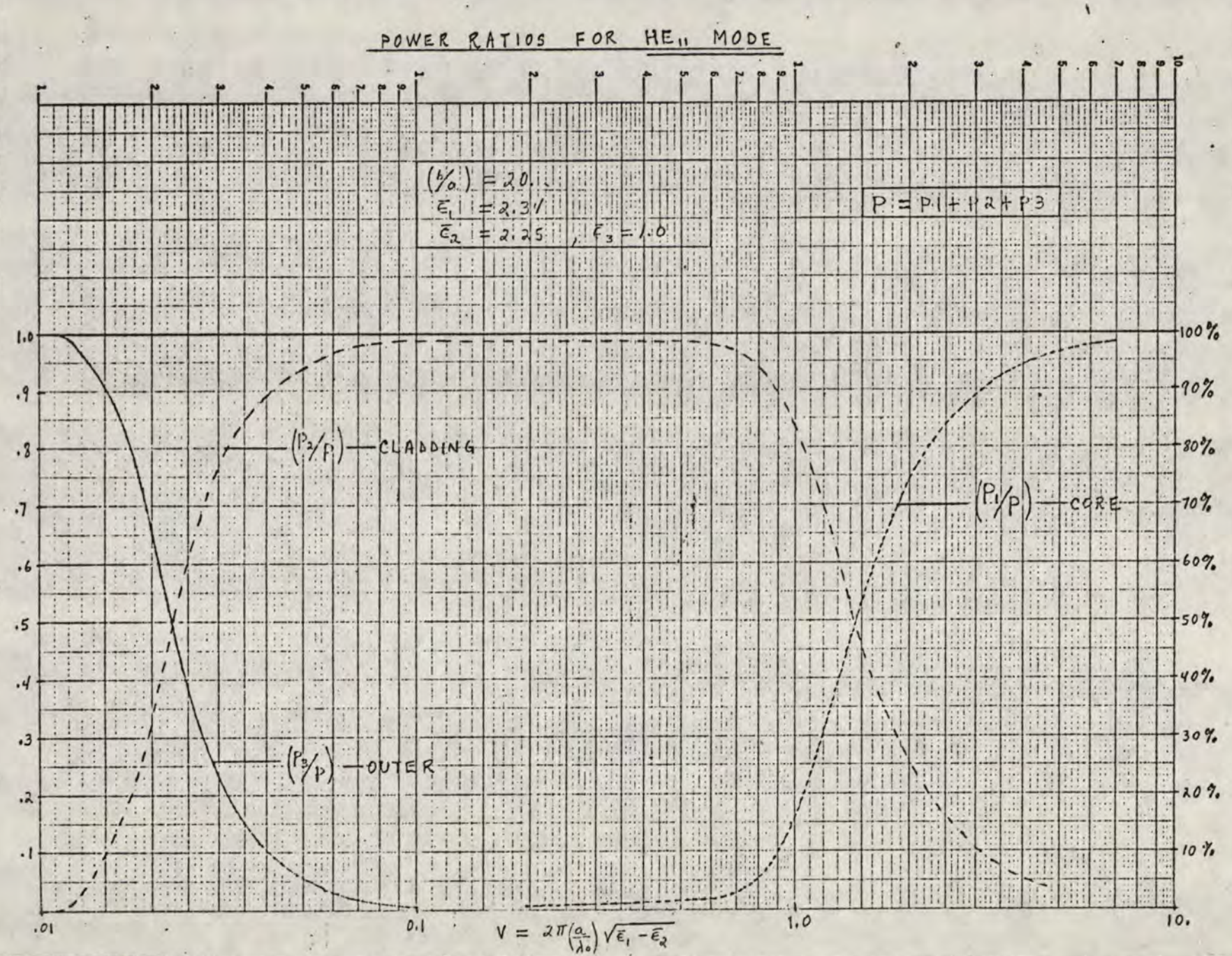
POWER RATIOS FOR HE11 MODE
(b/a) = 2.0
ε1 = 2.31
ε2 = 2.25 , ε3 = 1.0
P = P1 + P2 + P3
(P2/P) — CLADDING
(P3/P) — OUTER
(P1/P) — CORE
1.0
.9
.8
.7
.6
.5
.4
.3
.2
.1
100%
90%
80%
70%
60%
50%
40%
30%
20%
10%
.01
0.1
1.0
10.
V = 2π(a/λ0)√(ε1 − ε2)

FIG. 9

5. Plots of Transverse Field Intensity (Electric).

Instead of plotting the six individual field components directly, we plot the transverse electric field intensity (E_t) - which is more of physical interest and will also be required in scattering study. The electric field intensity is given by $E_t = \sqrt{E_r^2 + E_\phi^2}$

(a) Hybrid Modes:

In Fig. 10 we show the radial field distributions (HE_{11}, EH_{11}, HE_{12}) for three $\bar{\beta}$ values.

1. Leaky Region: (i) near cut-off - $\bar{\beta} = 1.101$

(ii) near transition - $\bar{\beta} = 1.505$

(b) Circularly Symmetric Modes:

Radial distribution of TE_{01} and TM_{01} is shown in Fig. 11 for two values of $\bar{\beta}$.

1. near cut-off: $\bar{\beta} = 1.101$
2. near transition: $\bar{\beta} = 1.498$

These radial plots clearly demonstrate that the field intensity in the cladding is very large for "leaky" modes, but for a propagating mode the field decays quite rapidly in the cladding (as expected).

TRANSVERSE FIELD INTENSITY vs. (r/a)

$E_t = \sqrt{E_r^2 + E_\phi^2}$

$(1/a) = 20.$
$\varepsilon_1 = 2.34$
$\varepsilon_2 = 2.25$
$\varepsilon_3 = 1.0$

CORE — CLADDING — OUTER

E_t

(HE_{11})
(EH_{11})
$[E_z (HE_{11})]$
HE_{12}
$|E_z| (HE_{11})$

NEAR CUT-OFF
$\bar{\beta} = 1.101$
LEAKY

(r/a)

HE_{11}
EH_{11}
HE_{12}

CORE — CLADDING — OUTER

$E_z (HE_{11})$

HE_{11}
HE_{12}

PROPAGATING REGION
$\bar{\beta} = 1.505$
FAR FROM CUT-OFF

TRANSVERSE FIELD INTENSITY vs. (r/a)

$E_t = \sqrt{E_r^2 + E_\phi^2}$

CORE — CLADDING — OUTER

E_t

HE_{11}
EH_{11}
HE_{12}
$|E_z| (HE_{11})$

(r/a)

FAR FROM CUT-OFF
$\bar{\beta} = 1.499$
LEAKY

$(1/a) = 20.$
$\varepsilon_1 = 2.34$
$\varepsilon_2 = 2.25$
$\varepsilon_3 = 1.0$

Fig. 10

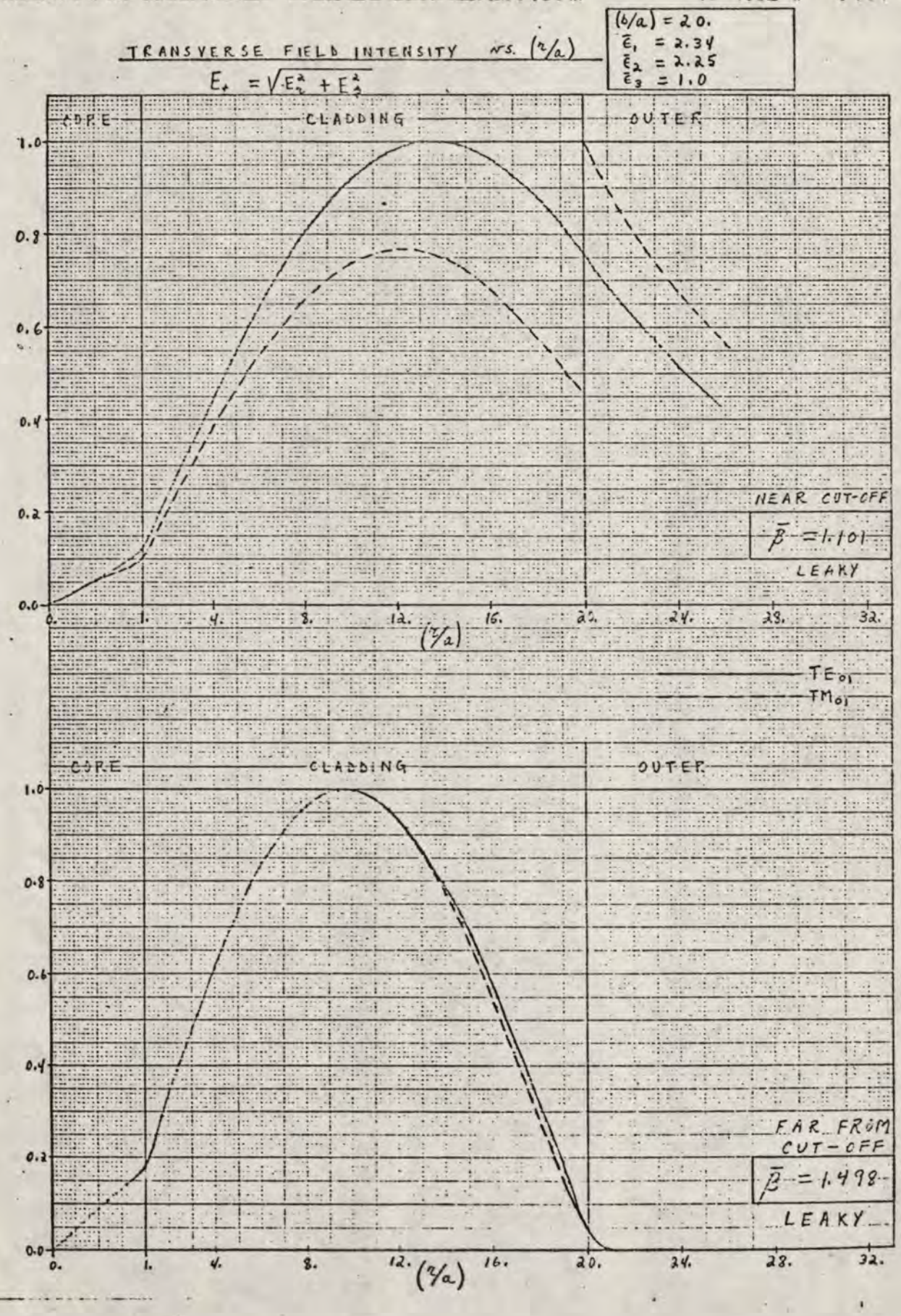
TRANSVERSE FIELD INTENSITY vs. (r/a)
$E_t = \sqrt{E_r^2 + E_z^2}$
(b/a) = 2.0.
$\bar{\epsilon}_1$ = 2.34
$\bar{\epsilon}_2$ = 2.25
$\bar{\epsilon}_3$ = 1.0
CORE
CLADDING
OUTER
1.0
0.8
0.6
0.4
0.2
0.0
0.
1.
4.
8.
12.
16.
20.
24.
28.
32.
(r/a)
NEAR CUT-OFF
$\bar{\beta}$ = 1.101
LEAKY
TE_{01}
TM_{01}
CORE
CLADDING
OUTER
FAR FROM CUT-OFF
$\bar{\beta}$ = 1.498
LEAKY

FIG. 11

PART II

LOSS CHARACTERISTICS OF CLADDED FIBRE

In arriving at the propagation characteristics of cladded fibre, we have assumed an ideal waveguide with an infinite axial length and no losses. The following losses[1-7] should be considered :

(1) Absorption Loss--caused mainly by metallic fibre impurities (e.g. Fe, Cu) which have their absorption band in the visible spectrum.

(2) Radiation and Mode Conversion Loss--caused by

(a) discrete scattering centres (dielectric fibre inhomogeneities such as cracks, crystallites, air bubbles etc).

(b) waveguide imperfections and bends.

Here, we focus attention on intrinsic fibre absorption loss and discrete scattering centres on the fibre axis.

1. ABSORPTION LOSS (due mainly to metallic fibre impurities)

Characterizing absorption loss by a complex permittivity ($\bar{\epsilon}_i = \bar{\epsilon}_i' - j\,\bar{\epsilon}_i''$, $i = 1, 2, 3$) in each region of the waveguide, we derived (in Report 1) an expression for the attenuation coefficient (assuming small losses*) given by

*NOTE : For the perturbation theory to be valid we require $\bar{\epsilon}_i'' << \bar{\epsilon}_i'$, i.e., $\tan \delta_i = \frac{\bar{\epsilon}_i''}{\bar{\epsilon}_i'} << 1$, since we are using unperturbed values of ($\bar{\beta}$, V) from the mode spectrum.

$$\alpha = \frac{\sum_{i=1}^{3} L_i}{2P_o} = \frac{\omega \sum_{i=1}^{3} [W_i(\bar{\beta}, V) \cdot \tan \delta_i]}{2 P_o(\bar{\beta}, V)} \qquad (2.1)$$

where

$P_o(\bar{\beta}, V)$ = total axial modal power launched at $z = 0$.

$W_i(\bar{\beta}, V)$ = total stored energy per unit length.

$\tan \delta_i = \frac{\bar{\epsilon}_i''}{\bar{\epsilon}_i'}$ = loss tangent for i^{th} region $\simeq 10^{-6} \quad 10^{-4}$.

$\simeq 10^{-6} \rightarrow 10^{-4}$

To keep the attenuation coefficient (α) valid for wide range of frequencies we normalize it with α_o, which is the attenuation coefficient of a plane wave propagating in an infinite medium having the same dielectric constant as the core ($\bar{\epsilon}_1 = \bar{\epsilon}_1' - j\bar{\epsilon}_1''$)

$$\alpha_o \simeq \frac{1}{2} \left(\frac{\omega}{v_o}\right) \left(\sqrt{\bar{\epsilon}_1'}\right) \tan \delta_1 \qquad (2.2)$$

$$\therefore \quad \left(\frac{\alpha}{\alpha_o}\right) = \frac{v_o \sum_{i=1}^{3} [W_i(\bar{\beta}, V) \tan \delta_i]}{\left(\sqrt{\bar{\epsilon}_1'}\right) \tan \delta_1 \cdot P_o(\bar{\beta}, V)} \qquad (2.3)$$

In Fig. 12, the normalized attenuation coefficient (α/α_o) for the first few modes is shown, where we have taken $\{\frac{\tan \delta_2}{\tan \delta_1} = 1.0, \tan \delta_3 = 0\}$.

Fig. 13 presents the same attenuation curves with the mode spectrum below for easy comparison.

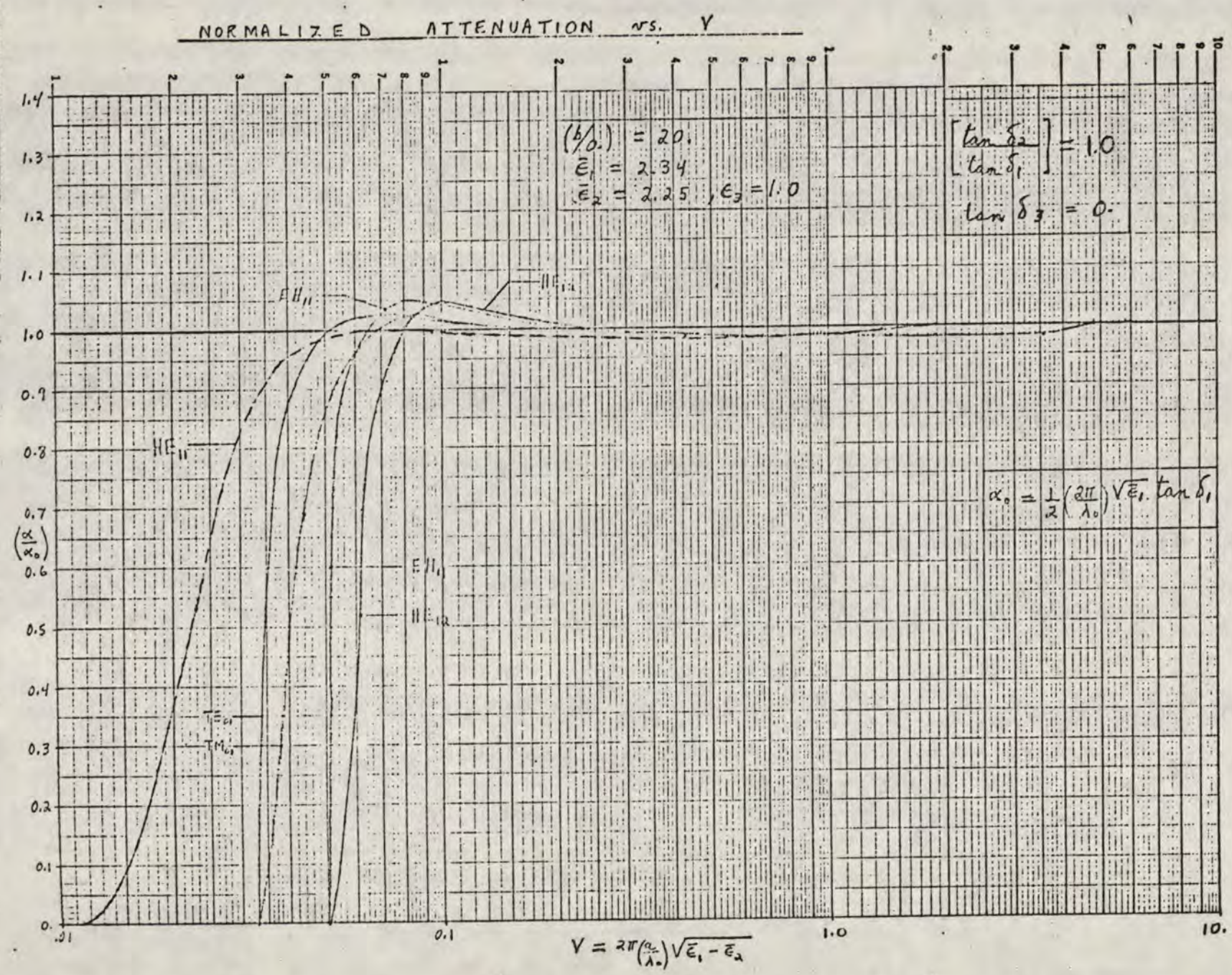
NORMALIZED ATTENUATION vs. V
(b/a) = 2.0
ε̄1 = 2.34
ε̄2 = 2.25 , ε3 = 1.0
[tan δ2 / tan δ1] = 1.0
tan δ3 = 0.
α0 = 1/2 (2π/λ0) √ε̄1 tan δ1
(α/α0)
V = 2π(a/λ0)√(ε̄1 − ε̄2)
HE11
EH11
HE12
EH12
TE01
TM01
1.4
1.3
1.2
1.1
1.0
0.9
0.8
0.7
0.6
0.5
0.4
0.3
0.2
0.1
0.
.01
0.1
1.0
10.

FIG. 12

NORMALIZED ATTENUATION vs. V

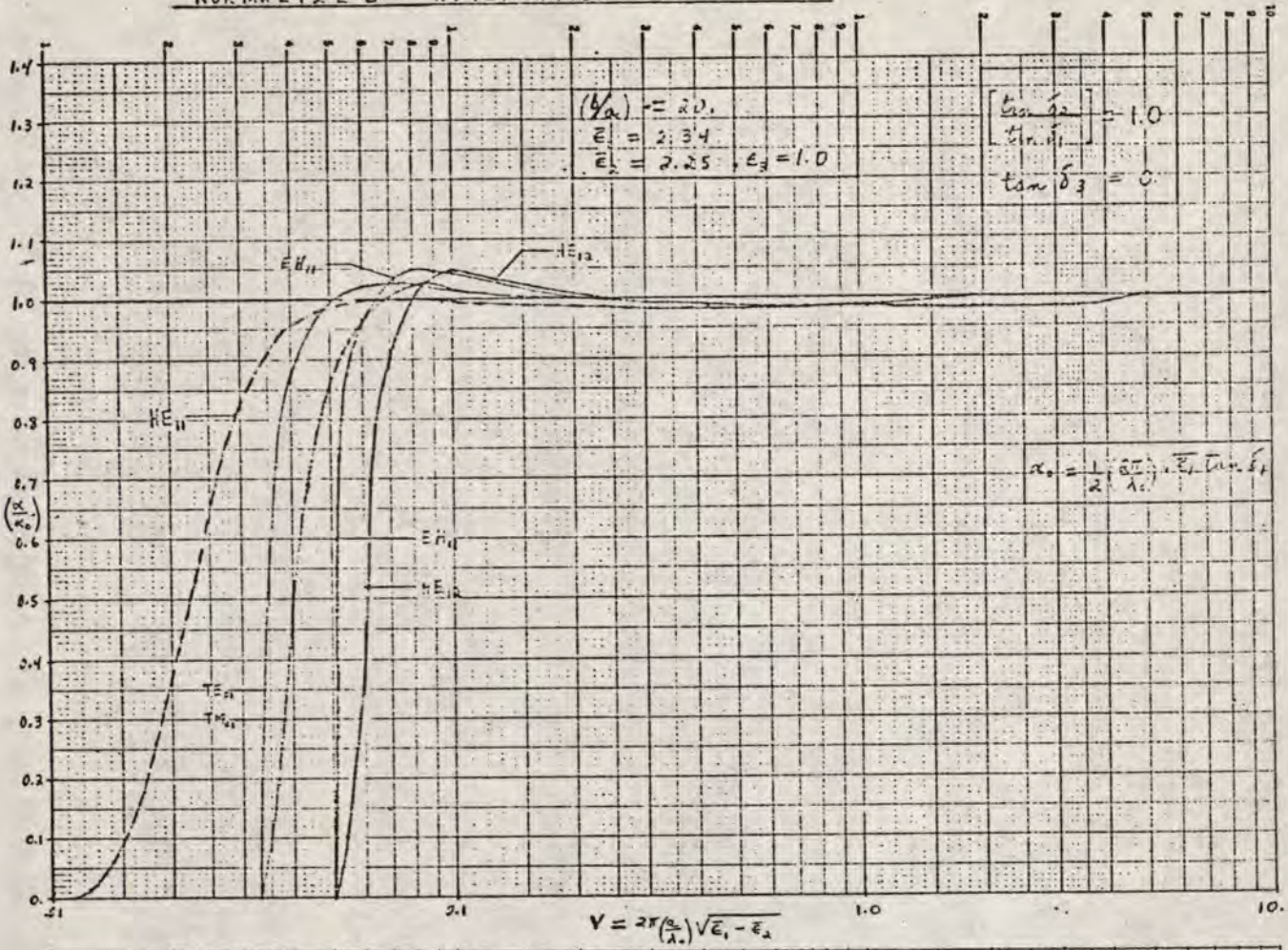

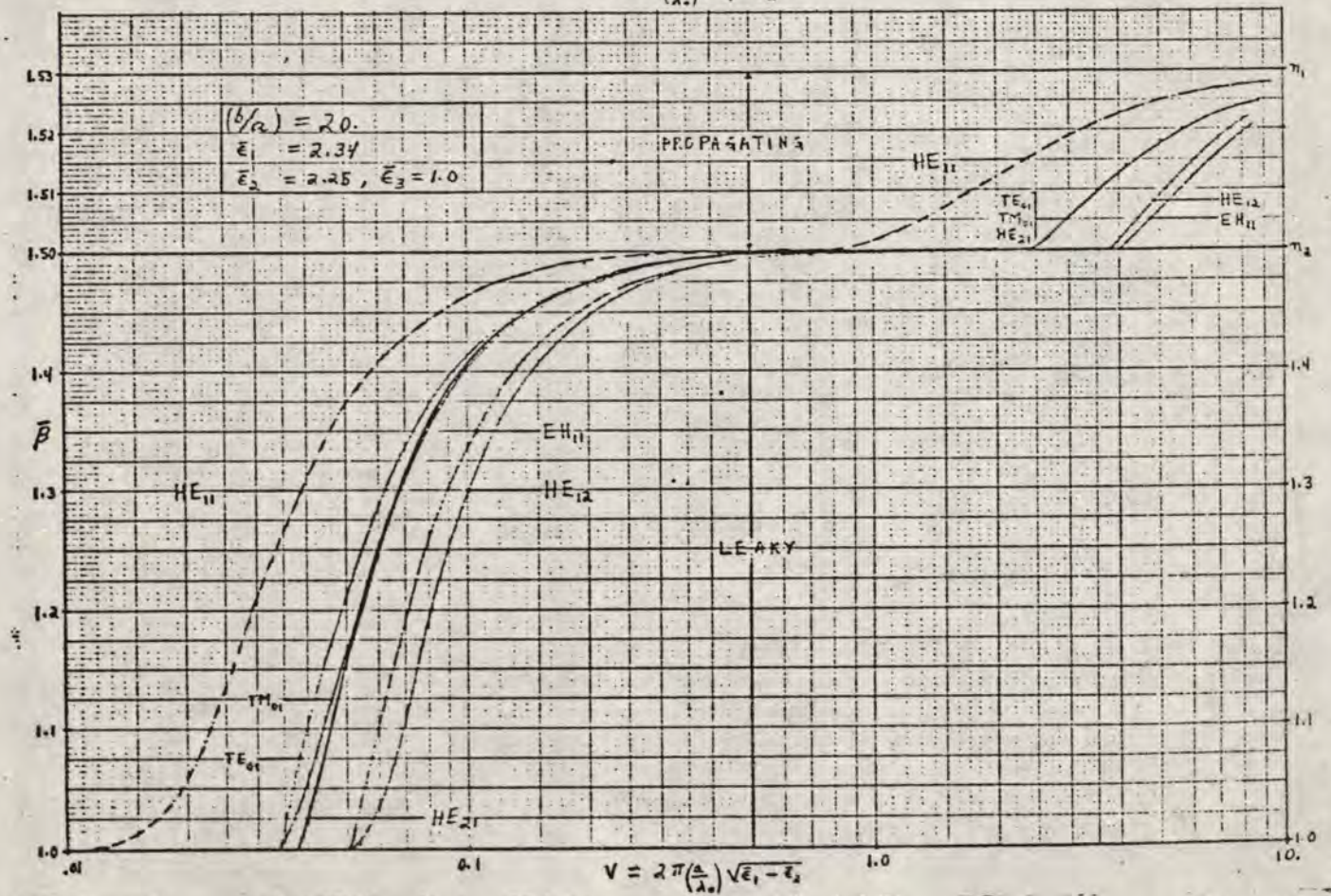

Fig. 13

It is observed that, as the power gets concentrated into the core, $(\frac{\alpha}{\alpha_o}) \to 1$, i.e., the attenuation coefficient of the waveguide behaves like that of bulk core medium.

2. Absorption Jacket (for mode control)

(a) Purpose and Design:

In order to support the thin fiber core ($\sim 2\mu$), as well as to protect it from its surroundings, a cladding is added on to it. But by introducing the finite cladding, a new type of guided modes is made possible, namely, "leaky" modes (or cladding modes).

To prevent "coupling" between "leaky" modes and the main information carrier (HE_{11} mode), it is necessary to attenuate any excited "leaky" modes before serious interference occurs.

Since the "leaky" modes have their energy and power concentrated in the cladding, these modes can be attenuated by applying a lossy coating to the cladding. The outer coating is referred to as the absorbing jacket, and will have a higher loss tangent ($\sim 10^{-4}$, 10^{-3} — black glass) than the cladding, which has intrinsic absorption loss. In practice, this is achieved by adding a thin layer of black glass on the cladding[7,8,9]. The black glass has a refractive index very close to that of the cladding,

so that one can consider the lossy layer as a part of the over-all cladding

thickness. Thus, in order to use our previous attenuation formula, we consider the cladding as made up of two regions:

(1) Inner Region: This has only intrinsic absorption loss ($\tan\delta \sim 10^{-5}, 10^{-6}$)

(2) Outer Region: This is the absorbing jacket which has a higher loss tangent ($\tan\delta \sim 10^{-4}, 10^{-3}$) than the inner region.

Fig. 14 illustrates the essential features of design.

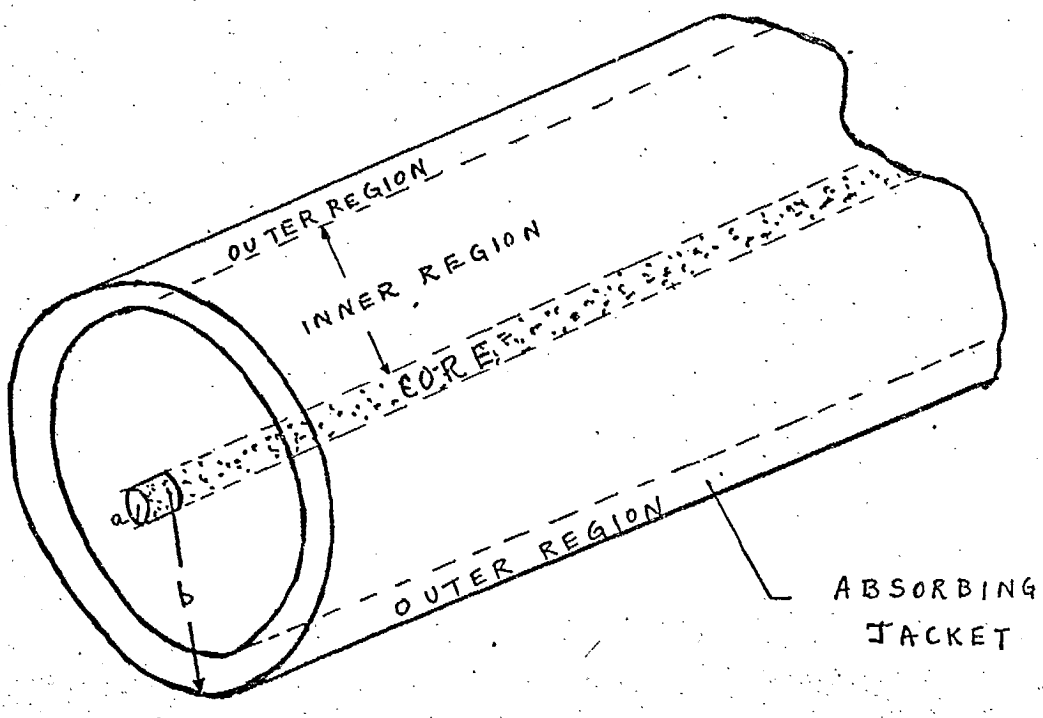

CORE: $\bar{\epsilon}_1 = \epsilon_1' - j\epsilon_1''$, $\tan\delta_1 = \dfrac{\epsilon_1''}{\epsilon_1'} \simeq 10^{-6}, 10^{-5}$

CLADDING:

(1) Inner Region: $\bar{\epsilon}_c = \bar{\epsilon}_2' - j\bar{\epsilon}_2''$, $\tan\delta_2 \simeq 10^{-6}, 10^{-5}$

(2) Outer Region: $\epsilon_{jk} = \bar{\epsilon}_2' - j f\bar{\epsilon}_2''$, $\tan\delta_{jk} \simeq 10^{-4}, 10^{-3}$

where $f \simeq 100$ (constant)

(b) Attenuation Formula

As stated in Section 1, the total attenuation coefficient is given by

$$\alpha \simeq \frac{\omega \sum_{i=1}^{3} [W_i(\bar{\beta}, V) \cdot \tan\delta_i}{2P_o(\bar{\beta}, V)}$$

For a particular region of the fibre waveguide we have

$$\alpha_i = \frac{L_i}{2P_o} = \frac{\omega W_i \tan\delta_i}{2P_o}, \text{ for the ith region.} \qquad (2.5)$$

Hence the attenuation for the absorbing jacket is given by

$$\alpha_{jk}^{(\text{jacket})} = \left(\frac{\omega}{2P_o}\right) W_{jk} \tan\delta_{jk}$$

$$= \frac{1}{2}\left(\frac{2\pi}{\lambda_o}\right)\left(\frac{v_o W_{jk}}{P_o}\right) \tan\delta_{jk}, \text{ using } \omega = \left(\frac{2\pi}{\lambda_o}\right) \cdot v_o \qquad (2.6)$$

NOTE: For perturbation theory to hold, the loss tangent of the absorption jacket must be small, i.e., $\tan\delta_{jk} = f\frac{\bar{\epsilon}_2''}{\bar{\epsilon}_2'} = f\tan\delta_2 << 1$. This requirement is met, since $\tan_{jk} \simeq 10^{-4}, 10^{-3}$ (Black Glass).

$$\therefore \quad (\alpha_{jk}a) = \frac{1}{2}\left(2\pi\frac{a}{\lambda_o}\right)\left(\frac{v_o W_{jk}}{P_o}\right) \cdot \tan\delta_{jk}$$

$$= \frac{1}{2}\frac{V}{(N.A.)}\left(\frac{v_o W_{jk}}{P_o}\right) \cdot \tan\delta_{jk} = \bar{\alpha}(\bar{\beta},V)\cdot\tan\delta_{jk} \tag{2.7}$$

where

$$V = \frac{2\pi a}{\lambda_o}(N.A.), \quad N.A. = \sqrt{\bar{\epsilon}_1 - \bar{\epsilon}_2}, \quad \text{Numerical Aperture}$$

and

$$\bar{\alpha}(\bar{\beta},V) \equiv \frac{1}{2}\frac{V}{(N.A.)}\left(\frac{v_o W_{jk}(\bar{\beta},V)}{P_o(\bar{\beta},V)}\right. \tag{2.8}$$

over a given fiber length L, the attenuation is then

$$ATTN\Big|_{nepers} = (\alpha_{jk}a)\cdot\left(\frac{L}{a}\right) = \bar{\alpha}\cdot\left(\frac{L}{a}\right)\cdot\tan\delta_{jk} \tag{2.9}$$

and

$$ATTN\Big|_{dB} = 4.34\ \left(ATTN\Big|_{nepers}\right)$$

$$= 4.34\ \bar{\alpha}\cdot\left(\frac{L}{a}\right)\cdot\tan\delta_{jk} \tag{2.10}$$

where

$$\bar{\alpha}(\bar{\beta},V) = \frac{1}{2}\frac{V}{(N.A.)}\left(\frac{v_o W_{jk}(\bar{\beta},V)}{P_o(\bar{\beta},V)}\right) \tag{2.11}$$

This is the quantity that we plot directly.

Fig. 14 shows the attenuation $(\bar{\alpha})$ of an absorbing jacket, $(\frac{1}{5})$ of the cladding thickness, as a function of normalized frequency (V). The calculations were carried out for a ratio $(b/a) = 5$, but similar results hold for a larger ratio, $(\frac{b}{a}) = 20$.

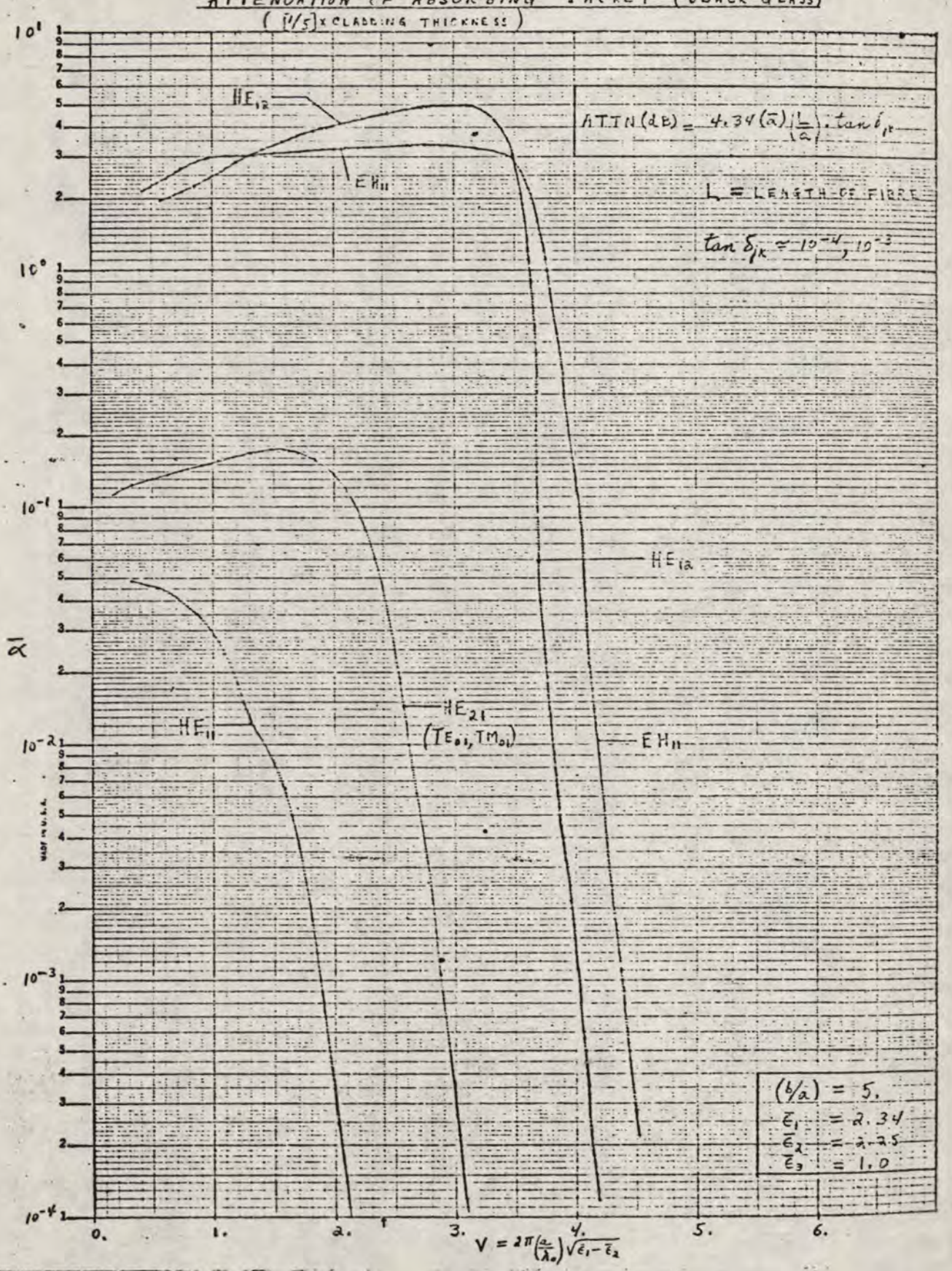
ATTENUATION OF ABSORBING JACKET (BLACK GLASS)
(b/a) x CLADDING THICKNESS
HE12
EH11
HE12
HE11
HE21
(TE01, TM01)
EH11
ATTN(dB) = 4.34 (ᾱ) (L/a) . tan δ1x
L = LENGTH OF FIBRE
tan δ1x ≈ 10⁻⁴, 10⁻³
(b/a) = 5.
ε̄1 = 2.34
ε̄2 = 2.25
ε̄3 = 1.0
ᾱ
V = 2π (a/λ0) √(ε̄1 − ε̄2)

FIG. 14

ATTENUATION OF ABSORBING JACKET

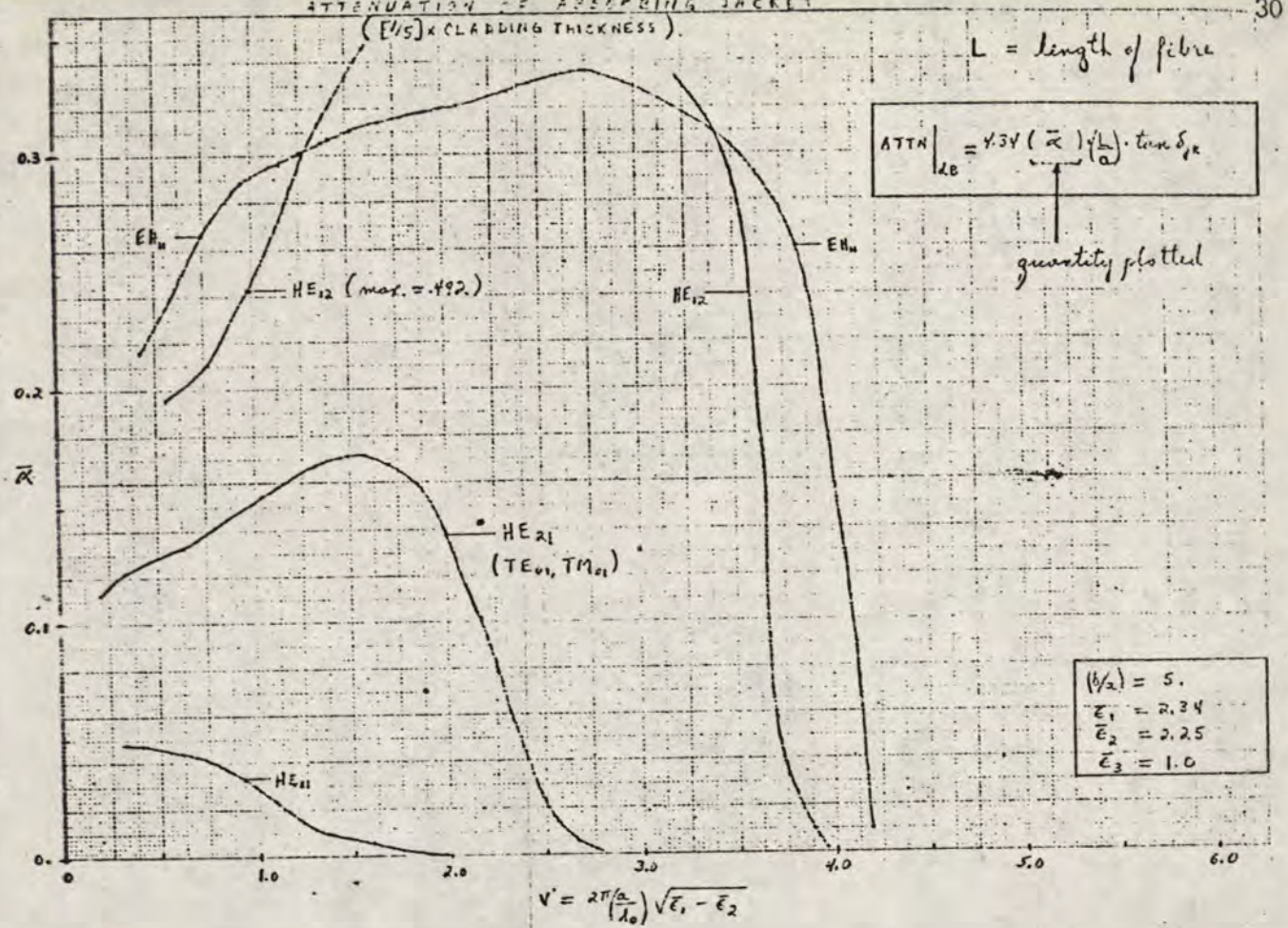

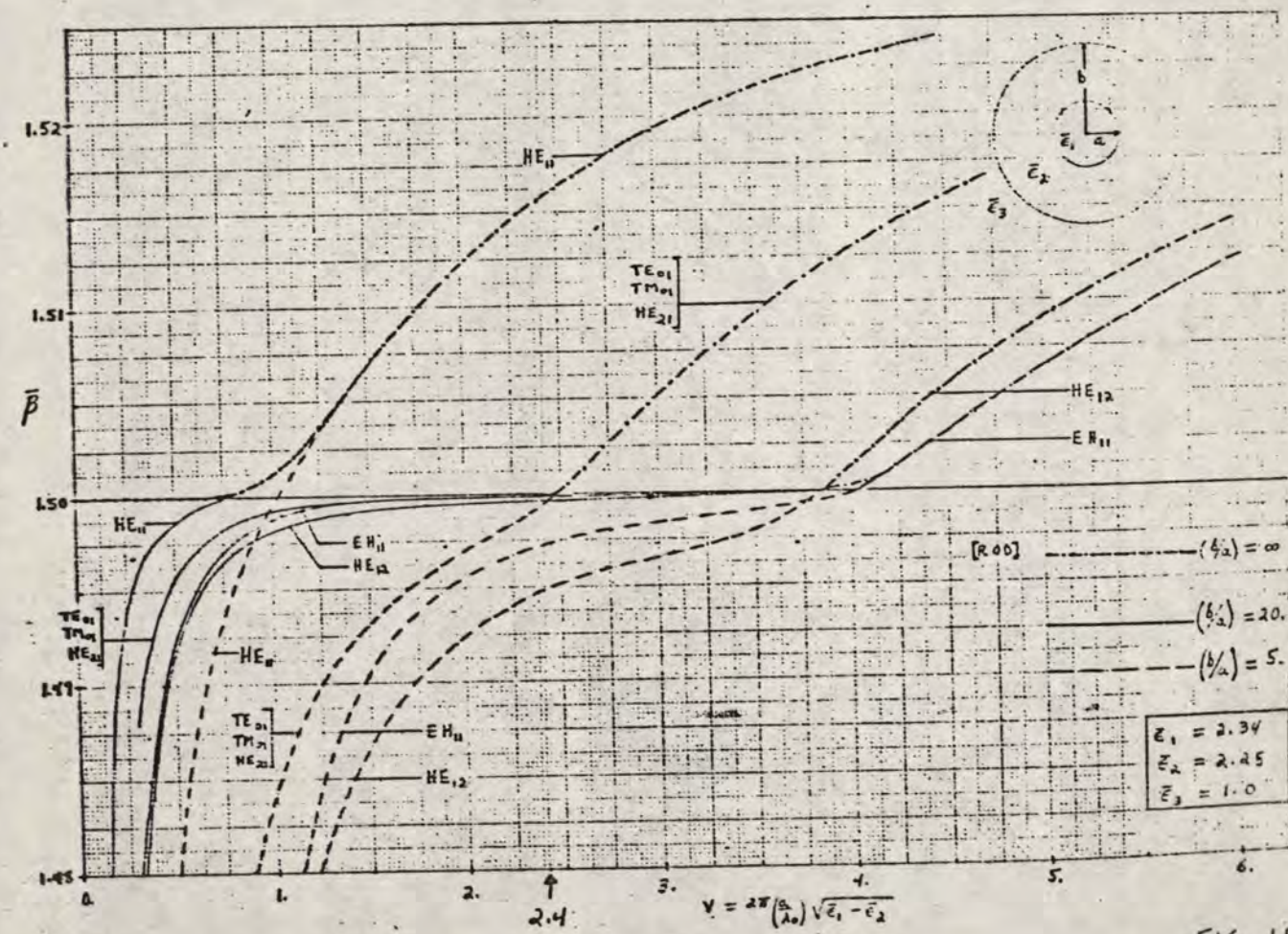

FIG. 15

In Fig. 15, we present the same attenuation curves (of the absorbing jacket) along with the mode spectrum for easy reference.

One can readily see from Fig. 15 that for single mode operation ($V \sim 2.4$), the higher order cladding modes [HE_{21}, TE_{01}, TM_{01}, EH_{11} HE_{12}] suffer much greater loss than the single core mode HE_{11}. Hence a good degree of "mode control" is achieved.

(c) Extension to Small Amplifications (Active Medium)

We realize that work is also being done in the other direction, i.e., where part or all of the cladding is made of an active medium[11] (pumped by laser). Here, the objective is to amplify the core modes ("propagating") by the evanescent wave interaction. This would be a first step in the design of a repeater. However, one must first attenuate any cladding modes ("leaky") to a very low level before the core modes are made to interact with the active medium; otherwise, the cladding mode would also be amplified, which is certainly an undesirable feature.

For small amplifications, one can use the same formula as for attenuation, except that now the loss tangent becomes negative, i.e.,

$$\text{For active medium} \left\{ \begin{array}{l} \bar{\epsilon} = \bar{\epsilon}' + j\bar{\epsilon}'' \\ \quad = \bar{\epsilon}' - j(-\bar{\epsilon}'') \end{array} \right\}, \tan\delta = -\frac{\bar{\epsilon}''}{\bar{\epsilon}'} \sim \begin{array}{l} 10^{-4} \\ 10^{-3} \end{array},$$

3. Power Lost from Scattering Centre (Fibre Impurity on or Very Near Fibre Axis

(a) Introduction

To get some insight into the attenuation due to scattering from fibre impurities or inhomogeneities, we focus attention on one scattering centre on or very near the fibre axis.

Consider the HE_{11} mode (fundamental mode of operation) incident on this scattering centre, which has an overall dimension very much smaller than the incident wavelength (Rayleigh theory)[12,13]. A current moment will be induced on the scattering centre, and this will scatter power into radiation and surface waves (both "leaky" and "propagating" modes).

Here we evaluate the fraction of power lost into radiation, some power will be scattered into higher order modes as well, but will not be considered. As mentioned earlier, one can "eliminate" the higher order "leaky" modes by using an absorbing jacket.

We note in passing that, for a random array (N) of scattering centres (on or very near fibre axis), which have a separation large compared to the wavelength, the total radiated power is then just N times that of a single particle, since there are no coherent phase relationships between light radiated by different particles. It seems that until now, no report has been

written on the distribution of these fibre impurities, so that a statistical approach would have to be used. Two papers relevant at this point are:

(1) "Loss Mechanisms and Measurements in Clad Glass Fibers and Bulk Glass". Ref. 3.

(2) "Measurement of the Angular Distribution of Light Scattered from a Glass Fiber Optical Waveguide". Ref. 9

(b) Fraction of Power Scattered in Radiation (Radiating Mode)

As depicted in Fig. 16, a fraction of the incident (HE_{11}) power is scattered into radiation. Earlier researchers[8] have estimated this radiation loss by assuming an infinite cladding and using the formula for power radiated in an infinite medium with core refractive index n_1 (since $n_1 \simeq n_2$).

We now present an exact solution, i.e., one which takes into account the finite cladding thickness. This is done through Green's function method and Fourier Transform technique[14]. Comparison between the approximate medium solution and the exact one is also made.

(i) Approximate Solution: infinite medium with $n_1 = \sqrt{\epsilon_1}$.

The power radiated by a small scattering centre (volume v', current moment I_m) in an infinite medium with refractive index n_1 ($= \sqrt{\epsilon_1}$ is given by

$$P^2 = \frac{1}{2} I_m^2 R_o \qquad (2.12)$$

FIG. 16

SCATTERING FROM A SMALL PARTICLE ON FIBRE AXIS

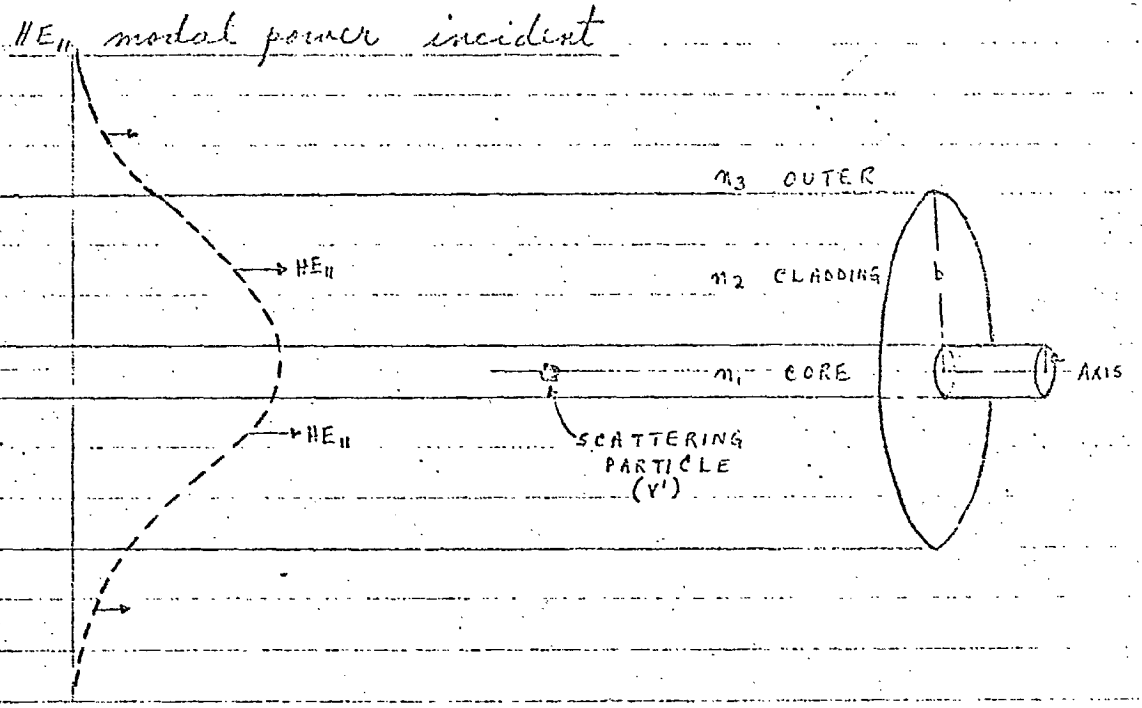

① —— RADIATING MODE
② —— "LEAKY" (OR CLADDING MODE)
③ —— "PROPAGATING" (OR CORE MODE)

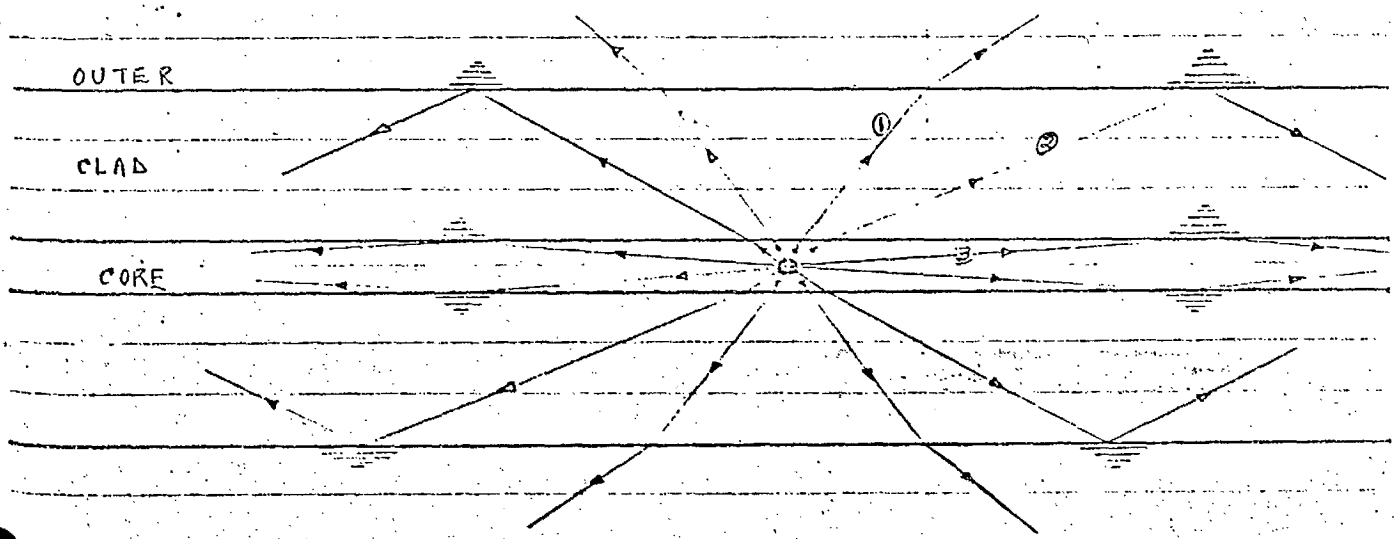

where

$$I_m \approx |\underline{J}| v' = \text{current moment} \tag{2.13}$$

$$R_o = \left(\frac{80\pi^2}{n_1}\right) \cdot \left(\frac{1}{\lambda_o^2}\right) = \text{radiation resistance of a point source in an infinite medium with } n_1 \tag{2.14}$$

Considering the two special cases of a dielectric (ϵ') or a metallic particle (σ) it can be shown that (See Appendix I)

$$|\underline{J}| = \omega \Delta \epsilon' |E_i'| A_1 \quad , \text{ for } \underline{\text{dielectric}} \text{ particle} \tag{2.15}$$

$$|\underline{J}| = \sigma |E_i'| A_1 \quad , \text{ for } \underline{\text{metallic}} \text{ particle} \tag{2.16}$$

where

$\Delta \epsilon = (\epsilon_1 - \epsilon')$

A_1 = excitation modal coefficient for HE_{11} mode

$|E_i'|$ = transverse field intensity at scattering centre

Let us find the ratio of radiated power between a <u>metallic</u> and a <u>dielectric</u> particle, with same scattering volume.

$$P^r_{metal} = \frac{1}{2}\left\{I^2_m|_{metal}\right\} R_r = \frac{1}{2}(\sigma |E_i| A_i v')^2 R_r \tag{2.17}$$

(R_r: Radiation Resistance)

$$P^r_{dielectric} = \frac{1}{2}\left\{I^2_m|_{diel.}\right\} R_r = \frac{1}{2}(\omega \Delta\epsilon |E_i'| A_1 v')^2 R_r \tag{2.18}$$

$$\therefore \quad \frac{P^r_{metal}}{P^r_{diel.}} = \left(\frac{\sigma}{\omega \Delta\epsilon}\right)^2 = \left\{\frac{\sigma \lambda_o Z_o}{2\pi \Delta\epsilon}\right\}^2 \tag{2.19}$$

which is just the ratio of the corresponding current moments and where

$$\bar{\epsilon} = (\bar{\epsilon}_1 - \bar{\epsilon}'), \quad Z_o \simeq 376.7.$$

Specific Example:

Consider scattering from a metallic particle (e.g. Cu, Fe) as compared to that of an air bubble in the fibre.

$$\sigma \simeq 10^7 \quad \{\sigma(\text{Cu}) = 5.8 \times 10^7,\ \sigma(\text{Fe}) = 1.0 \times 10^7\}$$

$$\Delta\bar{\epsilon} = (2.34 - 1.0) = 1.34$$

$$\lambda_o = 0.9\,\mu \quad (\text{Ga As Laser})$$

$$\therefore \quad R \equiv \frac{P^r_{\text{metal}}}{P^r_{\text{diel.}}} = \left(\frac{10^7 \times (9 \times 10^{-7})(376.7)}{(6.28)(1.34)}\right)^2 \simeq 14.2 \times 10^4$$

$$R\,(\text{dB}) = 10 \log_{10}(14.2 \times 10^4) = 55.2 \text{ dB}$$

This clearly shows the reason for large scattering loss when the fibre has a large quantity of metallic impurities.

(ii) Exact Method (Green's Function Solution)

$$P_r = \frac{1}{2} I_m^2 R_r \qquad (2.20)$$

where

$I_m = |J|v' = \omega \epsilon |E_i'| A_1 v'$ for dielectric particle

R_r = radiation resistance of a point source on fibre axis (evaluated by Green's function method, see Appendix II.)

Normalizing the power radiated by the HE_{11} incident modal power and scattering $(\bar{\epsilon}', v')$ parameters we get on setting

$$P_i(HE_{11}) = \pi b^2 \bar{S}_i(V) A_1^2, \quad V = 2\pi \left(\frac{a}{\lambda_o}\right)\sqrt{\bar{\epsilon}_1 - \bar{\epsilon}_2} \tag{2.21}$$

where the full expression for P_i has been given in Report No. 1.

(iii) Approximate Solution: infinite medium $(n_1 = \sqrt{\bar{\epsilon}_1})$

$$\frac{P^r}{P_i(\Delta\bar{\epsilon}\,\bar{v}')^2} = \frac{C^4}{2\pi Z_o^2} \cdot \frac{V^2}{(\bar{\epsilon}_1 - \bar{\epsilon}_2)} \left\{\frac{|E_i'|^2}{\bar{S}_i(V)}\right\} \cdot \bar{R}_o(V) \tag{2.22}$$

(iv) Exact Solution: (Green's Function Method)

$$\frac{P^r}{P_i(\Delta\bar{\epsilon}\,\bar{v}')^2} = \frac{C^4}{2\pi Z_o^2} \cdot \frac{V^2}{(\bar{\epsilon}_1 - \bar{\epsilon}_2)} \left\{\frac{|E_i'|^2}{\bar{S}_i(V)}\right\} \cdot \bar{R}_r(V) \tag{2.23}$$

where

$$\bar{R}_o(V) = b^2 R_o \qquad \bar{R}_r(V) = b^2 R_r \qquad \left| \quad C = a/b, \quad Z_o = \sqrt{\frac{\mu_o}{\epsilon_o}} \right. \tag{2.24}$$

and

$\Delta\bar{\epsilon} = (\bar{\epsilon}_1 - \bar{\epsilon}')$, $\bar{v}' = \left(\frac{v'}{a^3}\right)$, normalized scattering volume

(c) Discussion of Scattering Results

Fig. 17(a) shows the variation of $\frac{R_r}{R_o} = \frac{P_r}{P_o}$ vs. $\Delta\bar{\epsilon}$ where $\Delta\bar{\epsilon} = (\bar{\epsilon}_1 - \bar{\epsilon}_2)$. This graph is to indicate that even when $\Delta\bar{\epsilon} \to 0$, one cannot use the radiation formula for an infinite core medium, since $\left(\frac{R_r}{R_o}\right)$ does not approach the value one.

Fig. 17(b) presents $(\frac{R_r}{R_o}) = (\frac{P_r}{P_o})$ vs. V. Here again $(\frac{R}{R_o})$ does not approach one as V increases; hence the infinite medium formula is not accurate.

The results of both Fig. 17(a) and 17(b) indicate that one cannot take the cladding to behave as an infinite medium when the power scattered into radiation is calculated.

Fig. 18 illustrates the fraction of scattered power into radiation. Both the exact and the approximate (infinite medium $n_1 = \sqrt{\epsilon_1}$) solution are shown. It is observed that difference between the two solutions can be as large as 5 dB.

The flattening of the curves for high frequency (V) is attributed to the saturation of HE_{11} modal power.

$(P_2/P_0) = (R_2/R_0)$ vs. $\Delta\bar{\epsilon}$ [SCATTERING CENTRE ON FIBRE AXIS]

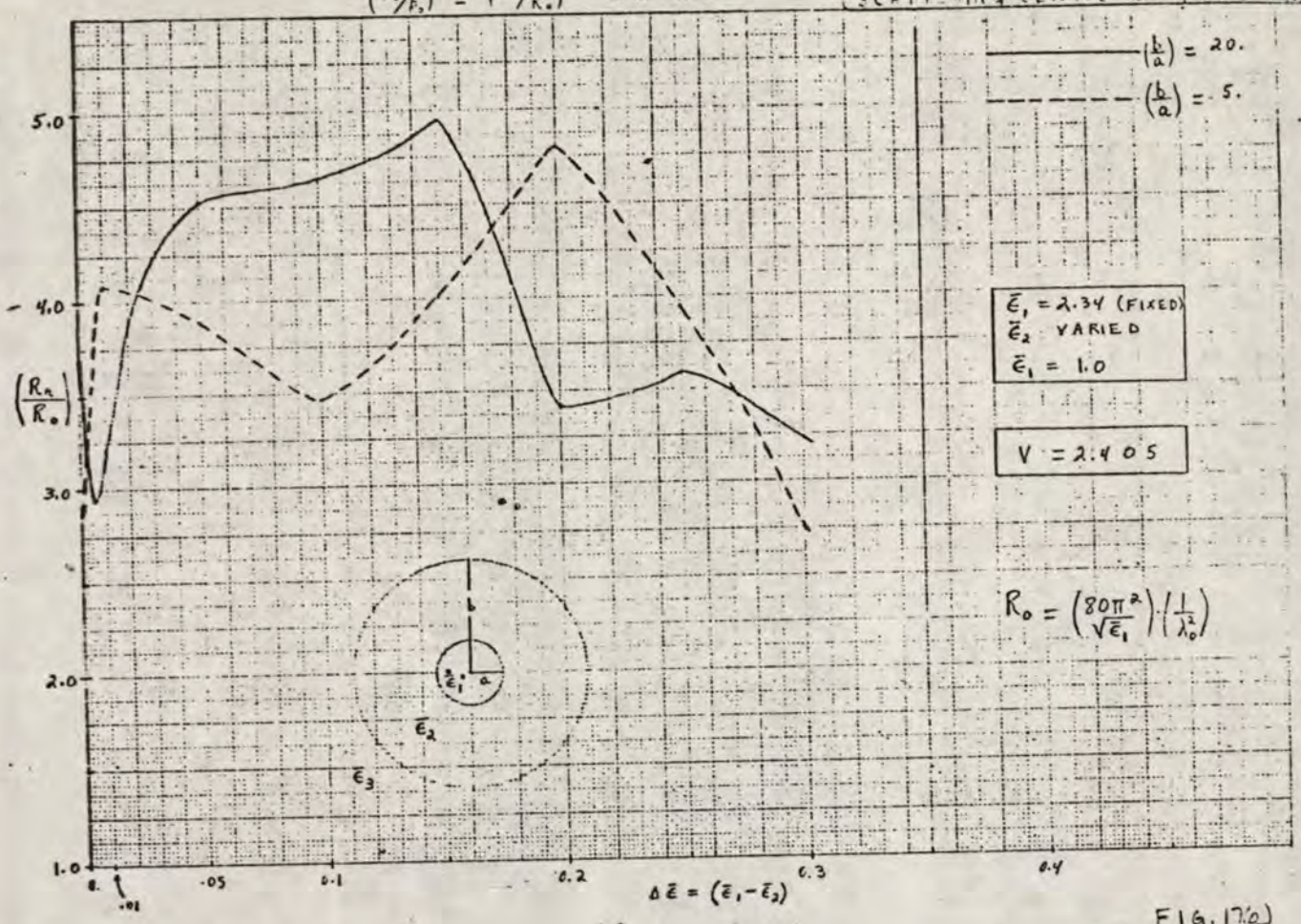

FIG. 17(a)

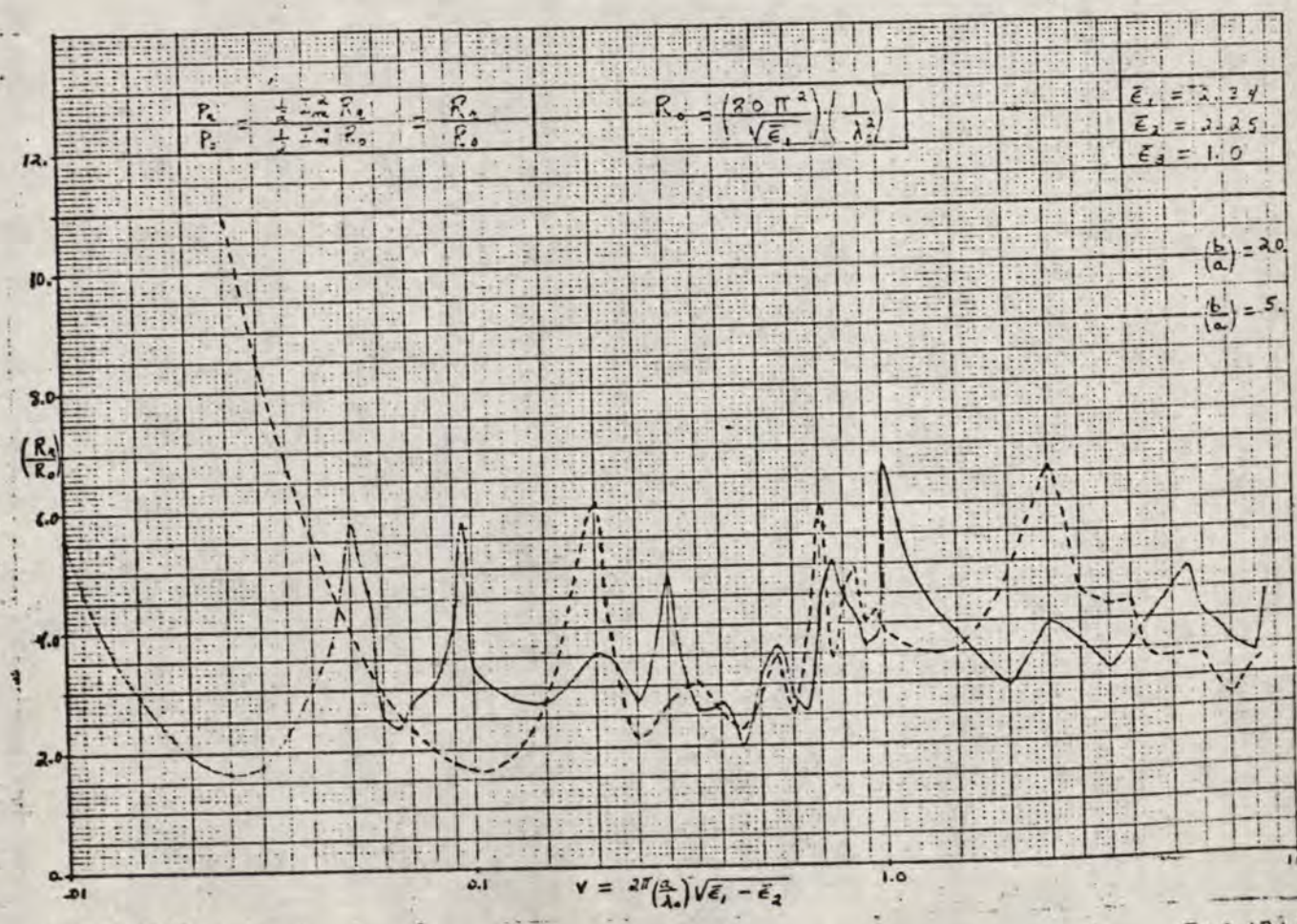

FIG. 17(b)

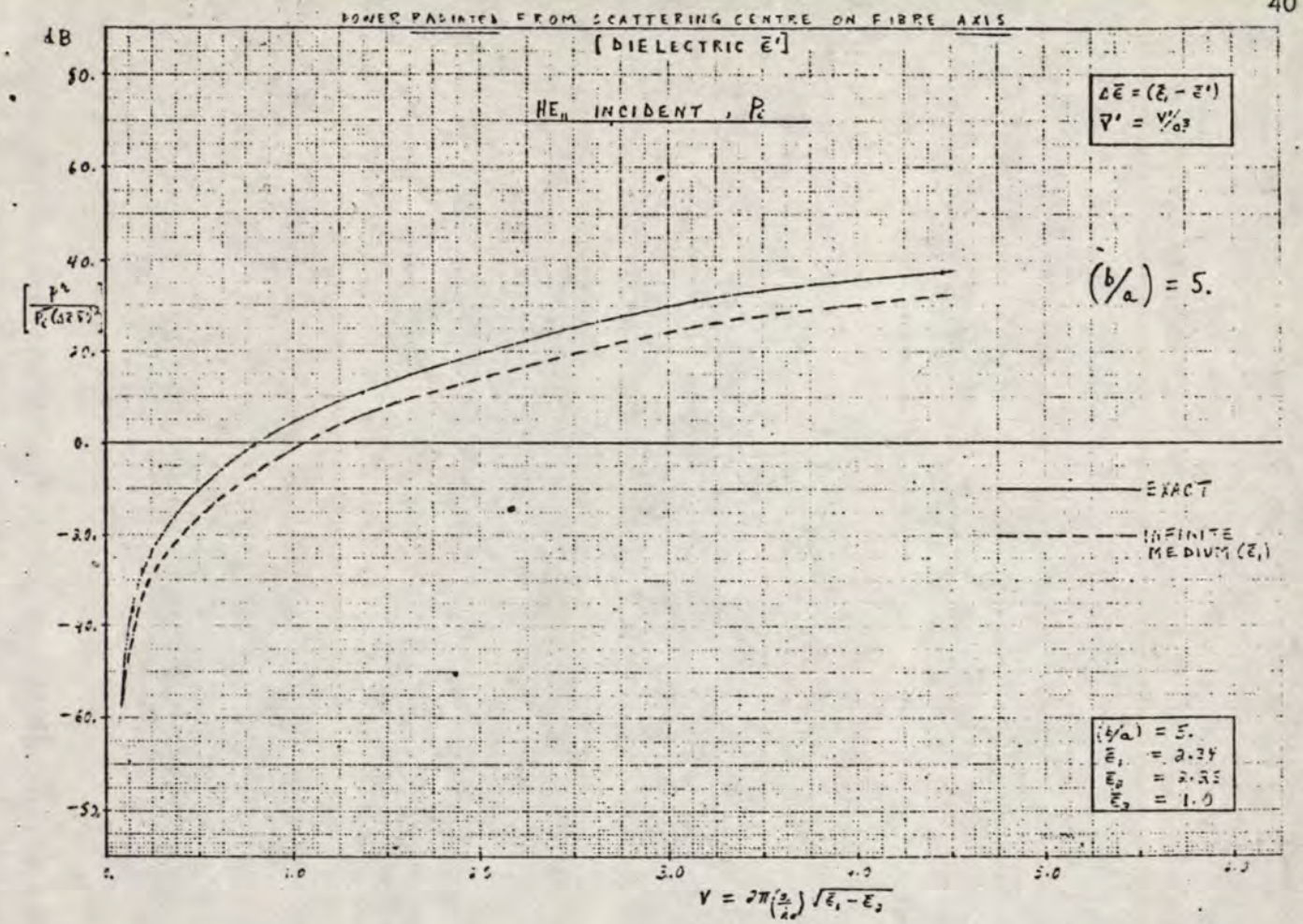
POWER RADIATED FROM SCATTERING CENTRE ON FIBRE AXIS
[DIELECTRIC $\bar{\varepsilon}'$]
HE_{11} INCIDENT, P_i
dB
$\Delta\bar{\varepsilon} = (\bar{\varepsilon}_1 - \bar{\varepsilon}')$
$\bar{V}' = V'/a^3$
$(b/a) = 5.$
$\left[\frac{P^s}{P_i(\Delta\bar{\varepsilon}\bar{V}')^2}\right]$
EXACT
INFINITE MEDIUM ($\bar{\varepsilon}_1$)
$(b/a) = 5.$
$\bar{\varepsilon}_1 = 2.34$
$\bar{\varepsilon}_2 = 2.25$
$\bar{\varepsilon}_3 = 1.0$
$V = 2\pi\left(\frac{a}{\lambda_0}\right)\sqrt{\bar{\varepsilon}_1 - \bar{\varepsilon}_2}$

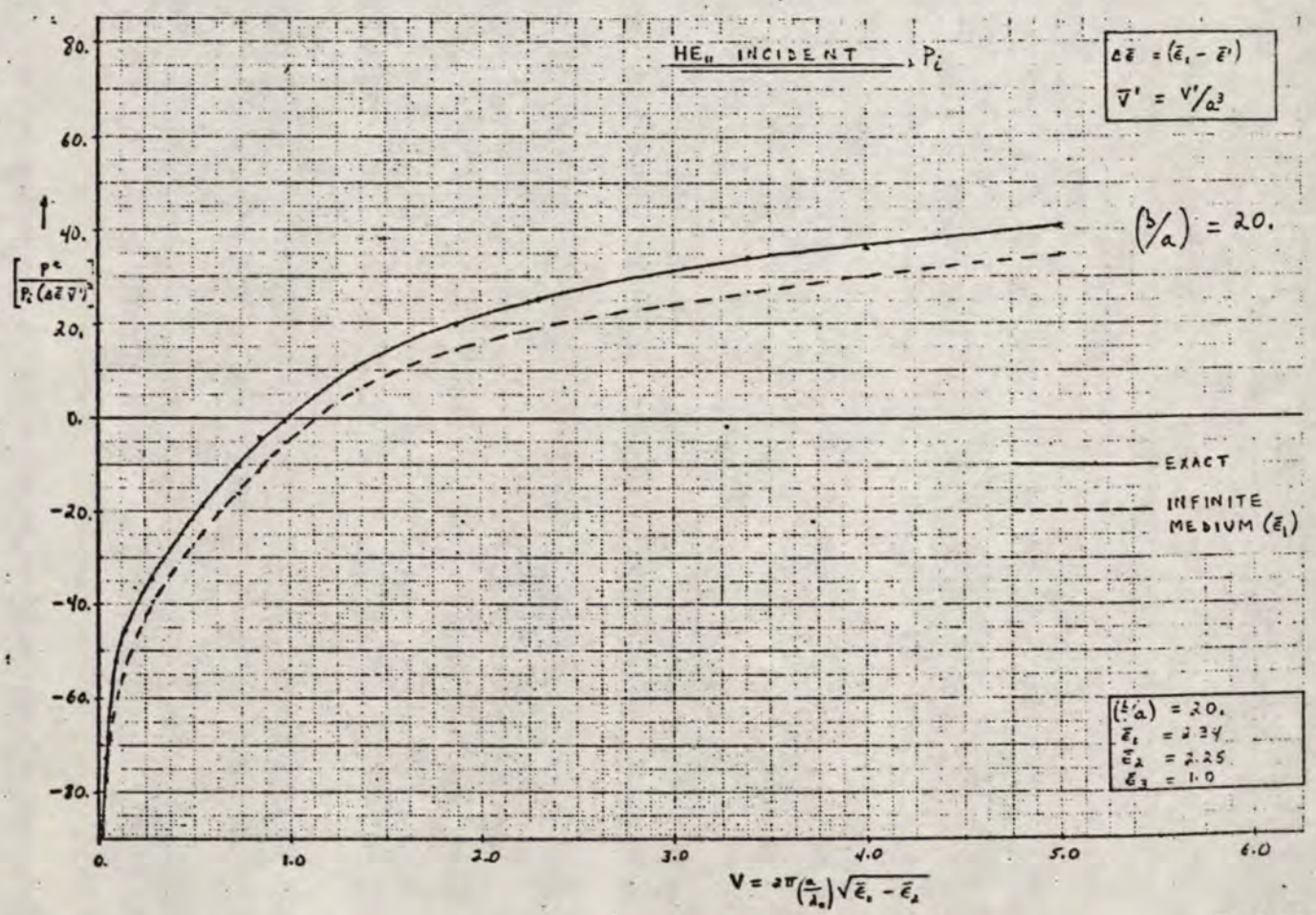
HE_{11} INCIDENT, P_i
$\Delta\bar{\varepsilon} = (\bar{\varepsilon}_1 - \bar{\varepsilon}')$
$\bar{V}' = V'/a^3$
$(b/a) = 20.$
$\left[\frac{P^s}{P_i(\Delta\bar{\varepsilon}\bar{V}')^2}\right]$
EXACT
INFINITE MEDIUM ($\bar{\varepsilon}_1$)
$(b/a) = 20.$
$\bar{\varepsilon}_1 = 2.34$
$\bar{\varepsilon}_2 = 2.25$
$\bar{\varepsilon}_3 = 1.0$
$V = 2\pi\left(\frac{a}{\lambda_0}\right)\sqrt{\bar{\varepsilon}_1 - \bar{\varepsilon}_2}$

FIG. 13

CONCLUSIONS

Propagation Characteristics for ideal and lossless cladded optical fibre waveguides have been presented. Calculations were carried out for a practical cladding to core ratio of 20 which is suitable for single mode operation. At the same time, effects of cladding thickness on the dispersion curves of the modes have also been examined.

Intrinsic absorption loss is accounted for by introducing a small negative imaginary part ("perturbation") to the dielectric permittivity in each region of the optical fibre waveguide. This yields attenuation curves for small absorption losses. A way of achieving mode control by using an absorbing jacket is also examined. Mention is also made to the research in amplification of the core modes by using an active cladding medium, where due consideration must be given to the presence of "leaky" (or cladding) modes.

A step towards evaluating the power loss from fibre scattering centres has been made. Concentrating on a small scattering particle on or very near the fibre axis, the power radiated is computed. The analysis should be extended to study the mode conversion problem.

APPENDIX 1

DERIVATION OF INDUCED CURRENT DENSITY ON A SCATTERING PARTICLE. (DIMENSION SMALLER THAN INCIDENT λ)

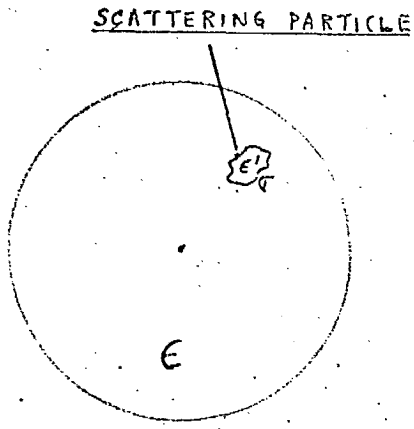

1. Dielectric Scattering Particle (ϵ')

Let (E_i, H_i) = fields without scattering particle

(E', H') = perturbed fields in presence of particle

$$\Delta\bar{\epsilon} = (\epsilon - \epsilon')$$

$\therefore$ Inside particle $\nabla \times \underline{H}' = (\sigma + j\omega\epsilon')\,\underline{E}'$

$$\simeq j\omega\epsilon'\underline{E}', \quad \therefore \sigma \simeq 0$$

$$= j\omega(\epsilon - \Delta\epsilon)E', \text{ using } \epsilon' = (\epsilon - \Delta\epsilon)$$

$$= (j\omega\epsilon\underline{E}') - (j\omega\Delta\epsilon\underline{E}') \qquad (1)$$

for small perturbations $(\underline{E}', \underline{H}') \simeq (\underline{E}_i, H_i)$

$\therefore$ we can write $\nabla \times \underline{H}_i = (j\omega\epsilon\underline{E}_i) - (j\omega\Delta\epsilon E_i) \equiv$

$$\equiv (j\omega\epsilon\underline{E}_i) + J_{diel} \qquad (2)$$

where

$$J_{diel} = -j\omega\Delta\epsilon\underline{E}_i \quad , \quad \underline{E}_i = \text{incident field}$$

$$\equiv |E_i|A_1$$

2. Metallic Scattering Particle (σ)

Here the displacement current ($j \omega \epsilon E'$) can be neglected

$$\therefore \quad \nabla X \underline{H}_i = \sigma \underline{E}_i = J_{metal} \tag{3}$$

$$\therefore \quad J_{metal} = \sigma \underline{E}_i \quad , \quad \underline{E}_i = \text{incident field}$$

$$= |E_i| A_1$$

APPENDIX II

EXPRESSION FOR RADIATION RESISTANCE OF A POINT SOURCE. FOURIER TRANSFORM TECHNIQUE AND GREEN'S FUNCTION SOLUTION

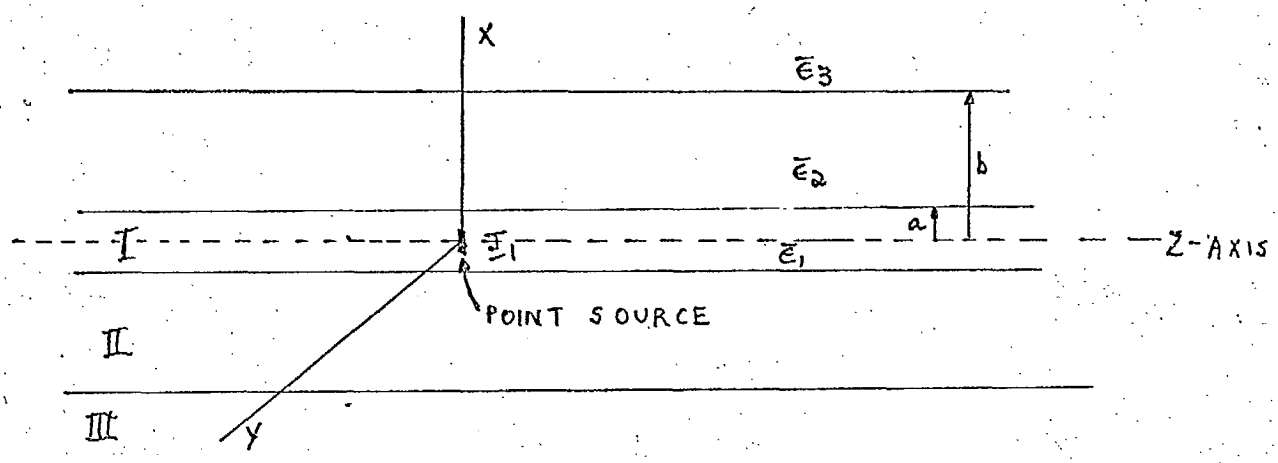

The current density is specified by

$$\underline{J}_1 = \frac{\hat{x}\, Je\, \delta(\rho)\, \delta(z)}{2\pi\rho} \qquad (1)$$

$$I_m \equiv \int \underline{J}_1 \, dv = Je = \text{Current Moment.}$$

REGION I: $0 \le \rho \le a$

$$\nabla X \underline{E} = i k_o H$$

$$\nabla X \underline{H} = -i k_o \underline{E} + \underline{J} \qquad (2)$$

where $(\underline{E}, \underline{H}, \underline{J})$ are normalized quantities.

Representing the actual fields as

$$f(\rho, \phi, z) = \frac{k_o}{2\pi} \int_{-\infty}^{\infty} \left[\sum_{n=-\infty}^{\infty} F(\rho, \gamma)\, e^{in\phi} \right] e^{ik_o \gamma z}\, d\gamma \qquad (3)$$

Fourier Transform Technique

transforms and decouples eqn. (2) to yield the wave equations for $\begin{Bmatrix} H_{z1} \\ E_{z1} \end{Bmatrix}$, namely

$$-\nabla_t^2 \begin{bmatrix} H_{z1}(\rho,\gamma) \\ iE_{z1}(\rho,\gamma) \end{bmatrix} + k_o^2 \eta_1^2 \begin{bmatrix} H_{z1}(\rho,\gamma) \\ iE_{z1}(\rho,\gamma) \end{bmatrix} = \frac{i}{2} Je\sqrt{\mu_o} \quad \frac{\partial}{\partial\rho}\left\{\frac{\delta(\rho)}{2\pi\rho}\right\}$$

$$\cdot\left\{\begin{bmatrix} -1 \\ \gamma/\bar{\epsilon}_1 \end{bmatrix} \cdot e^{i\phi} \quad + \begin{bmatrix} 1 \\ \gamma/\bar{\epsilon}_1 \end{bmatrix} \cdot \quad e^{-i\phi}\right\} \tag{4}$$

where $\eta_1 = \sqrt{\bar{\epsilon}_1 - \gamma^2}$. Eqn. (4) clearly reveals that only $n = \pm 1$ modes will be excited.

Equation (4) also holds in Regions II and III where $Je = 0$, $n_1 \rightarrow n_2 = \sqrt{\bar{\epsilon}_2 - \gamma^2}$, $n_3 = \sqrt{\bar{\epsilon}_3 - \gamma^2}$ respectively. The solutions in each region are given by

REGION I: (Green's function solution, for point source)

$$\begin{aligned} i E_{z1,n}(\rho,\gamma) &= I\eta_1 \left[T_n H_1(k_o \eta_1 \rho) + A_n J_1(k_o \eta_1 \rho) \right] \\ H_{z2,n}(\rho,\gamma) &= I\eta_1 \left[S_n H_1(k_o \eta_1 \rho) + B_n J_1(k_o \eta_1 \rho) \right] \end{aligned} \tag{5}$$

REGION II: (source free solution)

$$\begin{aligned} iE_{z2,n}(\rho,\gamma) &= I\eta_2 \left[E_n Y_1(k_o \eta_2 \rho) + F_n J_1(k_o \eta_2 \rho) \right] \\ H_{z2,n}(\rho,\gamma) &= I\eta_2 \left[C_n Y_1(k_o \eta_2 \rho) + D_n J_1(k_o \eta_2 \rho) \right] \end{aligned} \tag{6}$$

REGION III: (source free solution)

$$iE_{z3,n}(\rho,\gamma) = I\eta_3 L_n H_1(k_o \eta_3 \rho)$$

$$H_{z3,n}(\rho,\gamma) = I\eta_3 \, G_n \, H_1(k_o \eta_3 \rho)$$

where $I = i\frac{Je}{4}\sqrt{\mu_o}$, $T_n = \frac{i\gamma}{2\epsilon_1}$, $S_n = \frac{in}{2}$

$(A_n, B_n, C_n, D_n, E_n, F_n, G_n, L_n)$ are amplitude coefficients determined by matching the tangential components at $\rho = a, b$. Using Maxwell's curl equations, the transverse components of the transformed $\underline{E}, \underline{H}$ fields can be expressed in terms of E_z, H_z.

The power radiated is

$$P_r = \frac{1}{2\sqrt{\mu_o \epsilon_o}} \operatorname{Re} \int_{-\infty}^{\infty} \int_{o}^{2\pi} \left[E_{\varphi 3}(\rho,\varphi,z) \, H^*_z(\rho,\varphi,z) \right.$$

$$\left. - E_{z3}(\rho,\varphi,z) \, H^*_{\varphi 3}(\rho,\varphi,z) \right] \rho \, d\varphi \, dz = \frac{k_o \rho}{2\sqrt{\mu_o \epsilon_o}} \sum_{n=\pm 1} \tag{8}$$

$$\operatorname{Re} \int_{-\infty}^{\infty} \left[E_{\varphi 3,n}(\rho,\gamma) H^*_{z3,n}(\rho,\gamma) - E_{z3,n}(\rho,\gamma) H^*_{\varphi 3,n}(\rho,\gamma) \right] d\gamma \tag{9}$$

using Parseval's Theorem

Now for $1 < |\gamma|$, the radial component of the complex Poynting vector is purely imaginary ("evanescent" waves); hence these do not contribute to the radiated power.

Making the usual far-field approximations, the radiated power reduces to

$$Pr = \frac{J_e^2}{2} Z_o \frac{k_o^2}{4\pi} \sum_{n=\pm 1} \int_{-1}^{1} \left[|G_n|^2 + |L_n|^2 \right] d\gamma \tag{10}$$

$$\equiv \frac{1}{2}(J_e^2) Rr \, , \quad Z_o = \sqrt{\frac{\mu_o}{\epsilon_o}}$$

$$\therefore \quad R_r = \frac{k_o^2}{4\pi} Z_o \sum_{n=\pm 1}^{+} \int_{-1}^{1} \left[|G_n|^2 + |L_n|^2 \right] d\gamma \qquad (11)$$

is the radiation resistance for a point source on fibre axis.

REFERENCES

1. F.P. Kapron, D.B. Keck and R.D. Maurer, "Radiation Losses in Glass Optical Waveguides", IEE Conf. 1970, No. 71, p. 148, 153.

2. D. Marcuse, "Radiation Losses of the Dominant Mode (HE_{11}) of Round Optical Fibres", ibid. p. 89-94.

3. A.R. Tynes, A. David Pearson, and D.L. Bisbee, "Loss Mechanisms and Measurements in Clad Glass Fibers and Bulk Glass", J. Opt. Soc. of Amer., Vol. 61, No. 2, Feb. 1971, p. 143-153.

4. A.W. Snyder, "Radiation Losses Due to Variations of Radius on Dielectric or Optical Fibers", IEEE Trans., MTT, Vol. 18, No. 9, Sept. 1970.

5. E.A.J. Marcatili, "Bends in Optical Dielectric Guides", B.S.T.J. (USA), Vol. 48, No. 7, p. 2103-32, Sept. 1969.

6. D. Marcuse, R.M. Derosier, "Mode Conversion Caused by Diameter Changes of Round Dielectric Waveguides", (also considers radiation loss), B.S.T.J. (USA), Vol. 48, No. 10, p. 3217-32, Dec. 1969.

7. R. Roberts, "Propagation Characteristics of Multimode Dielectric Waveguides at Optical Frequencies", IEE Conf. 1970, No. 71, p. 34-44.

8. P.J.B. Clarricoats and K.B. Chan, "Excitation and Propagation of Modes of a Multilayer Fibre", Electronics Letters, Vol. 6, No. 23, Oct. 1970.

9. Eric G. Rawson, "Measurement of the Angular Distribution of Light Scattered from a Glass Fiber Optical Waveguide", Applied Optics, Vol. 11, No. 11, Nov. 1972, p. 2477-2481.

10. A.W. Snyder, "Excitation and Scattering of Modes on a Dielectric or Optical Fiber", IEEE Trans. MTT Vol. MIT-17, No. 12, Dec. 1969.

11. K.O. Hill, A. Watanabe, and J.G. Chambers, (CRC) "Evanescent-Wave Interactions in an Optical Wave-Guiding Structure", Applied Optics, Vol. 11, No. 9, Sept. 1972, p. 1952-1959.

12. Born and Wolf, "Principles of Optics", Sec. 13.5, (4th ed.) 1970.

13. H.C. van de Hulst, "Light Scattering by Small Particles", Ch. 9, 10, 1957.

14. G.L. Yip, "Launching Efficiency of the HE_{11} Surface Wave Mode on a Dielectric Rod", IEEE Trans. MTT, Vol. 18, No. 12, Dec. 1970, p. 1033-1041.

MAY 29 1973
Rec'd ADMR
#281